Renewable and Sustainable Energy Reviews 34 (2014) 430–452

Contents lists available at ScienceDirect

Renewable and Sustainable Energy Reviews

journal homepage: www.elsevier.com/locate/rser

Absorption heat transformers – A comprehensive review

Kiyan Parham [a,*], Mehrdad Khamooshi [a], Daniel Boris Kenfack Tematio [a], Mortaza Yari [b], Uğur Atikol [a]

[a] Department of Mechanical Engineering, Eastern Mediterranean University, Gazimagusa, North-Cyprus, via Mersin 10, Turkey
[b] Faculty of Engineering, Department of Mechanical Engineering, University of Mohaghegh Ardabili, Ardabil 179, Iran

ARTICLE INFO

Article history:
Received 16 September 2013
Received in revised form
13 February 2014
Accepted 12 March 2014
Available online 31 March 2014

Keywords:
Absorption heat transformers
Single stage
Double stage
Working fluids
Crystallization
Industrial applications

ABSTRACT

In recent years, the use of absorption heat transformers (AHTs) has reached a remarkable edge. AHTs have great potential in the utilization and upgrading of low-level heat sources. These are typically waste heat obtained from industrial processes and those supplied from solar and geothermal sources. Other benefits of absorption cycles include using significantly less electricity, potentially having less CO_2 emission, causing no ozone layer depletion, and using natural refrigerants; and these contribute to increasing the attractiveness of these machines. The use of absorption heat transformers has become even more popular as the cost of fossil fuel continues to rise. In the present work, a comprehensive literature review has been carried out on AHTs, their applications, crystallization risk, working fluids, as well as performance evaluation by applying different models and economic aspects.

© 2014 Elsevier Ltd. All rights reserved.

Contents

1. Introduction

A heat transformer is a device which can deliver heat at a higher temperature than the temperature of the fluid by which it is fed. Absorption heat transformer systems are attractive because they use waste heat from industrial processes and renewable energy sources such as solar and geothermal. In addition, they can be used to upgrade low temperature waste heat to that of higher temperatures to be employed in a secondary process. The integration of AHTs with different thermodynamic cycles plays an important role in recovering the heat rejected by them or even increasing the energy efficiency of the whole system. There is a great number of review papers about absorption refrigeration systems [1–3]; yet to the best of the authors' knowledge, there is no work on the review of absorption heat transformers (AHTs). Therefore, this review shall help in filling this gap, and this paper will discuss the major issues related to AHTs. Firstly, single and double effect absorption heat transformers will be considered. Then, applications of AHTs and the working fluids utilized in them will be reviewed. Finally, risk analysis methods for crystallization in AHTs and economic aspects will be considered.

* Corresponding author. Tel.: +90 533 8761435; fax: +90 392 3653715.
E-mail address: kiyan.parham@emu.edu.tr (K. Parham).

http://dx.doi.org/10.1016/j.rser.2014.03.036
1364-0321/© 2014 Elsevier Ltd. All rights reserved.

Principally, the absorption heat transformers can be configured to be single stage absorption heat transformers (SAHTs), double stage and double effect absorption heat transformers (DAHTs), or triple absorption heat transformer (TAHTs).

The present work will substantially review the advances in SAHTs and DAHTs in the subsequent sections. Since TAHTs have been introduced only recently, hence the references that can be found on them are limited [4].

2. Single stage AHTs

Fig. 1 shows the general schematic of the absorption heat transformer in single stage mode. The SAHT basically consists of an evaporator, a condenser, a generator, an absorber, and a solution heat exchanger (SHE). The generator and evaporator are supplied with waste heat at the same temperature, leading to increased heat that can be collected at the absorber [5]. The AHT performs in a cycle which is the reverse of that of an absorption heat pump [6].

Refrigerant vapor is produced at state 4 in the evaporator by low or medium-grade heat source. The refrigerant vapor dissolves and reacts with the strong refrigerant-absorbent solution that enters the absorber from state 10, and the weak solution returns back to the generator at state 5.

The heat released from the absorber will be higher than the input heat in generator and evaporator due to the exothermic reaction of LiBr and water in it. In the generator, some refrigerant vapor is removed from the weak solution to be sent to the condenser and, consequently, the strong solution from the generator is returned to the absorber. After condensing the vaporized refrigerant in the condenser, it is pumped to a higher pressure level as it enters the evaporator. The waste heat delivered to the evaporator causes its vaporization. Again, the absorber absorbs the refrigerant vapor at a higher temperature. Therefore, the absorption cycles have the capability of raising the temperature of the solution above the temperature of the waste heat [7].

Kurem and Horuz [6] analyzed the absorption heat transformers using ammonia–water and water–lithium bromide solutions. Their results showed that the AHT system using H_2O/LiBr solution performed better than the system using ammonia water solution. Although water–lithium bromide solution was well suited for use in AHTs, it still had some disadvantages, namely corrosion, high viscosity, limited solubility, and a practical upper temperature limit. Horuz and Kurt [8] investigated an industrial application of the AHT system to obtain hot process water. For this purpose, the industrial textile company which had waste heat sources at $90 \pm 2\,^{\circ}C$ $(4 \times 15\ t/h)$ and required hot water for process at $120\,^{\circ}C$ was chosen. In the first case, in a basic single AHT, the waste heat was supplied to the generator and absorber at the same time (Fig. 2). The second used system had such a configuration that the waste hot water was directed first to the evaporator and then to the generator (Fig. 3). In the third system, in addition to the waste hot water configuration of the second system, an absorber heat exchanger was included instead of the solution heat exchanger (Fig. 4).

Finally, the last configuration incorporated the second and third systems with the addition of a refrigerant heat exchanger at the evaporator inlet (Fig. 5).

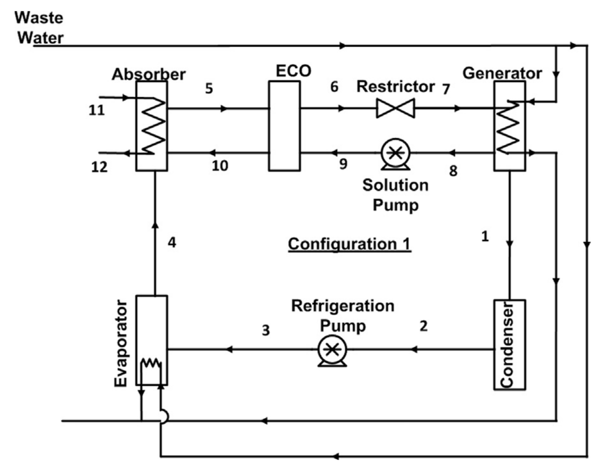


Fig. 2. Schematic diagram of SAHT (S-Type I) [8] (redrawn by authors).

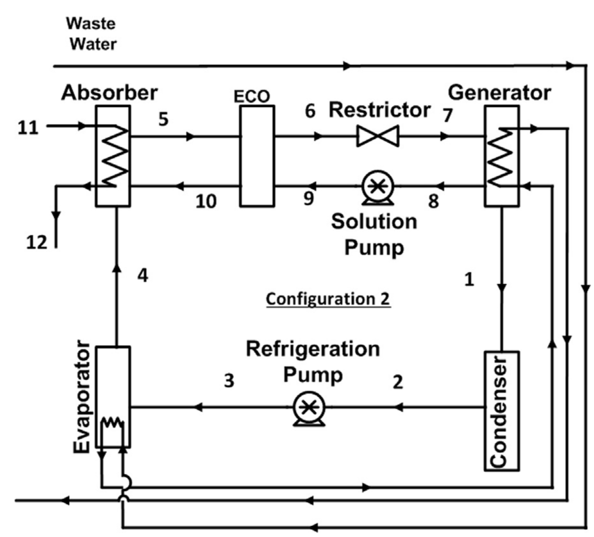


Fig. 3. Schematic diagram of SAHT (S-Type II) [8] (redrawn by authors).

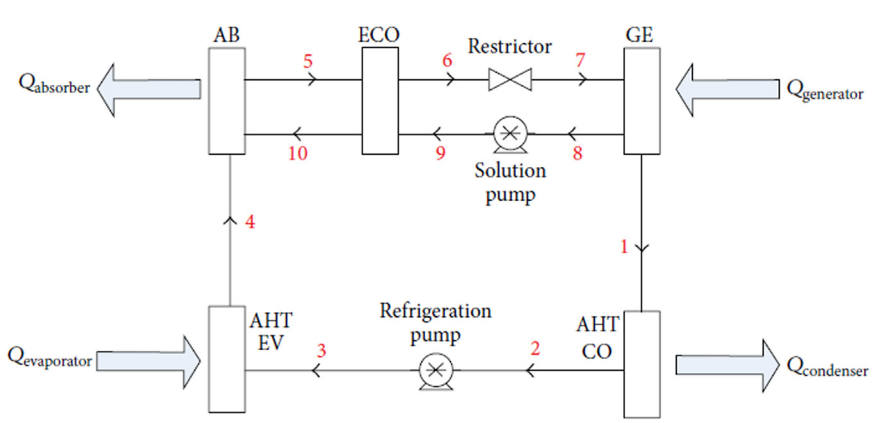


Fig. 1. Single stage absorption heat transformer [6].

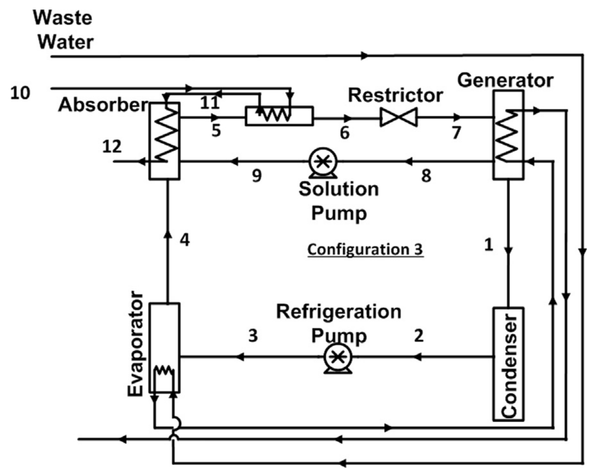


Fig. 4. Schematic diagram of SAHT (S-Type III) [8] (redrawn by authors).

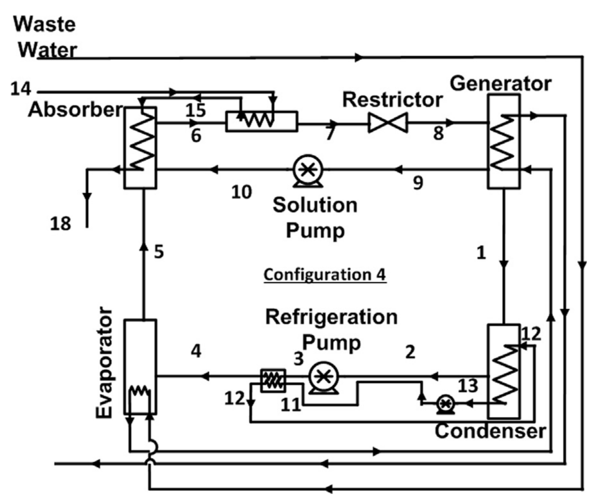


Fig. 5. Schematic diagram of SAHT (S-Type IV) [8] (redrawn by authors).

It is shown that, while the condenser temperature increases, the COPs and the absorber heat capacity decrease.

On the other hand, as the evaporator and the generator temperatures increase, so do the COPs and the absorber heat capacity. Additionally, it is proved that, when the evaporator temperature is higher than the generator temperature, the COP and the absorber heat capacity increase (Types II–IV).

In fact the latter is the most important result of Ref. [8] and this leads to the motivation of proposing Configurations (II–IV).

Ma et al. [9] reported the first industrial-scale heat transformer by recovering waste heat from a synthetic rubber plant which was used to heat water from 95 to 110 °C with heat flow of 5000 kW, obtaining a mean coefficient of performance (COP) of 0.470, and gross temperature lift of 25 °C. Furthermore, in this work, economic analyses were performed given a simple payback period of 2 years.

Sotelo and Romero [10] compared the performance and GTL of an absorption heat transformer with plate heat exchangers using water/Carrol to one using H_2O/LiBr. It was proved that water/Carrol mixture had a better performance and higher temperature lifts. Zhang and Hu [11] investigated the performance of a new working pair: H_2O+[EMIM] [DMP], in an AHT, and compared the simulation results to those of H_2O/LiBr and TFE/E181. It was concluded that, due to the fact that H_2O+[EMIM][DMP] has an excellent cycle performance, together with the advantages of negligible vapor pressure, no possibility of crystallization, and also having a weaker corrosion tendency to iron–steel materials, compared to the aqueous solution of lithium bromide, it could be used for industrial applications.

Zebbar et al. [12] elaborated a mathematical model for a H_2O/LiBr AHT to optimize those parameters having a significant effect on the endo-irreversible cycle for an existing heat transformer with already dimensioned total heat exchangers area. This optimization was achieved through the structural bond analysis of the heat transformer using the coefficient of structural bond (CSB) and varied parameters such as pressure (P) of the AHT, and solution concentration (X). Results showed that the irreversibility of the absorber and generator played a large role on the total system's entropy generated in case of varying concentrations, while when the pressure was varied the generator and condenser were the critical parameters. Moreover, at an optimal pressure ratio of 0.72, a COP of 0.486 was achieved instead of 0.479.

Rivera et al. [13] studied the performance of a single-stage heat transformer operating with the water/lithium bromide and the water/Carrol™ mixtures, theoretically and experimentally. It was observed that almost the same tendencies and values of the coefficient of performance and flow ratio are obtained in general for both mixtures; however, because of the higher solubility of the water/Carrol™ mixture, the SSHT operated over a large range of generator and evaporator temperatures, and with higher gross temperature lifts. Because the water/Carrol™ mixture has higher solubility than water/lithium bromide, and high experimental values were obtained for the gross temperature lift, they concluded that it could be a better alternative mixture to be used in absorption heat transformers.

In another work, Rivera and Cerezo [14] used additives 1-octanol and 2-ethyl-1-hexanol in a 2 kW single-stage heat transformer utilizing H2O/LiBr and operating at absorber temperatures ranging between 70 and 110 °C. The results showed that at the same conditions, absorber temperatures increased about 5 °C by adding 400 ppm of 2-ethyl-1-hexanol to the lithium bromide mixture. Also, it was shown that the coefficient of performance increases by up to 40% with the same additive.

Second law analysis of the latter mentioned work was done far ahead by the same team [15]. Their results demonstrated that for absorber temperatures between 84 and 88 °C, the highest COP, COPEXT, and ECOP are obtained with the use of the 2-ethyl-1-hexanol (400 ppm) additive, reaching values of up to 0.49, 0.40, and 0.43, respectively. The lowest coefficients of performance and the highest irreversibility rates were obtained using the single water/lithium bromide mixture. It was found that 2-ethyl-1-hexanol decreases the irreversibility considerably in the absorber, thereby increasing the efficiency of this component, and hence of the entire equipment.

Thermodynamic design data for absorption heat transformers without utilizing heat exchanger and with operation of different working fluids have been proposed by several researchers [16–23]. (More information is available in Table 1.)

Sozen and Yucesu [24] proposed a single stage absorption heat transformer that uses an ejector before the absorber as illustrated in Fig. 6. The results demonstrated that a reduction of 12% and 10% exergy losses is possible in the absorber and generator, respectively. Sozen [25] developed a mathematical model for simulating the performance of an AHT system with NH_3/water as working fluid and that is powered by a solar pond. The maximum upgrading of the solar pond's temperature by the AHT is obtained at 51.5 °C, with a gross temperature lift at 93.5 °C, and with coefficients of performance of about 0.4. The maximum temperature of the useful heat produced by the AHT was approximately 150 °C. The exergy analysis demonstrated that the non-dimensional exergy loss in the absorber was about 70%, while in the generator it was above 10–20%, and in the condenser it increased with an increase in condenser temperature.

Table 1
Single stage absorption heat transformer.

Configuration	T_{eva} (°C)	T_{gen} (°C)	T_{con} (°C)	T_{abs}(°C)	Working pair	*f*	GTL (°C)	COP	Heat source	Remarks	Reference
(S-Type I)	80	80	25	130	H_2O/LiBr	9.51	50	0.48	Waste heat from a cogeneration system in a textile company	While the T_{con} increases the COPs and the Q_{abs} decrease	[18]
(S-Type II)	80	73	25	130	H_2O/LiBr	18.63	50	0.46	Waste heat from a cogeneration system in a textile company	*Less COP than that of S-Type I*Q_{abs} and produced hot water increased by 81.1% and 2.81%	[18]
(S-Type III)	80	73	25	130	H_2O/LiBr	18.63	50	0.53	Waste heat from a cogeneration system in a textile company	Increase in COP and *f*	[18]
(S-Type I)	90	90	35	130	H_2O/LiBr		~3–30	0.494		Higher COP but crystallization is a problem	[21]
(S-Type I)	90	90	35	130	[EMIM][DMP]		~3–30	0.481	–	No Crystallization, COP and ECOP lower than H_2O+LiBr but higher than that of TFE+E181	[21]
(S-Type I)	90	90	35	130	TFE-E181		~3–30	0.458		COP and ECOP is lowest compared to H_2O+LiBr and TFE+E181	[21]
(S-Type IV)	80	73	25	130	H_2O/LiBr	18.63	50	0.55	Waste heat from a cogeneration system in a textile company	*14.1%, 158.5% and 3.59% increase in COP, Q_{abs} and produced hot water compared to S-Type I	[18]
(S-Type I)	70–80	70–80	25–30		H_2O/LiBr	–	Max GTL ≈ 42°c	Max COP ≈ 0.5	–	–	[23]
(S-Type I)	70–80	70–80	25–30		H_2O-Carrol	–	Max GTL ≈ 52°c	Max COP ≈ 0.47	–	Higher GTL than that of H_2O–LiBr, less corrosivity.	[23]
(S-Type I)	Q_{eva}=420, 425 W	Q_{gen}=446, 496 and 523 W	-	80–87	H_2O/LiBr + (1-octanol)	–	–	0.10–0.21	–	The additive increases slightly the T_{abs} and COP	[24]
(S-Type I)	Q_{eva}=420, 425 W	Q_{gen}=446, 496 and 523 W	-	83–92	H_2O/LiBr+ (2-ethyl-l-hexanol)	–	–	0.14–0.26	–	The additive increases considerably the performance of the system	[24]
(S-Type I)	30–70	30–90	10–50	40–120	Ammonia–water		1.43–18.6	0.024–0.454		COP decreases while the flow ratio increases with an increase in absorber temperature.	[26]
(S-Type I)	30–90	30–90	10–50	50–150	H_2O -carrol		2.86–81.87	0.218–0.495		The use of heat transfer additives in order to achieve high heat and mass transfer rates in the absorber must be emphasized when using more viscous absorbent mixtures as Carrol	[27]
(S-Type I)	30–90	40–90	10–50	60–140	Ammonia–sodium thiocyanate		3.81–20.9	0.001–0.507		The rate of COP increase depends on the absorber temperature when the generator temperature is increased from a lower temperature level than the evaporator temperature.	[28]
(S-Type I)	30–90	50–90	10–50	70–140	Ammonia–lithium nitrate		3.22–27.16	0.013–0.509		Higher COP at lower absorber temperature	[29]
(S-Type I)	30–80	40–80	10–50	50–100	Water–calcium chloride		4.94–101.96	0.023–0.512		The sensitivity of decrease in COP is greatest at the lower level of the waste heat temperature	[30]
(S-Type I)	30–70	40–90	10–50	60–100	Water–lithium chloride		2.59–22.23	0.172–0.510		The COP of the system in low temperature is higher than H_2O–LiBr and H_2O–LiCl	[31]
(S-Type I)	30–90	30–90	10–50	50–150	Aqueous-ternary hydroxide		3.32–97.14	0.106–0.504		The rate of decrease in COP is higher for higher condenser temperature	[33]
(S-Type I)	58	58	20	~150	H_2O–NH_3	93.5		0.4	Solar pond	The maximum temperature of the useful heat produced by the AHT was ~150	
(S-Type I)	70	70	30	85–112	H_2O/LiBr	3–8	–	0.43–0.485	–	–	[35]
(EAHT)	58	58	20	150	H_2O–NH_3	97.5		0.5	Solar pond	Pressure recovery and pre-absorption in the ejector improves the efficiency of the AHT.	[36]
(EAHT)	70	70	30	90–117	H_2O/LiBr	3–9	–	0.43–0.49	–	Higher useful delivered temperature and better performance	[34]
Vertical falling film AHT (Fig. 8)	70–85	70–85	25–35	90–110	H_2O/LiBr	20–25		~0.43-~0.48	Hot water	New approach leads to a significantly higher COP and exergy efficiency under off-design conditions	[36]
(S-Type I)	80	80	25	130	H_2O/LiBr	9.51	50	0.48	Waste heat from a cogeneration system in a textile company	While the T_{con} increases, the COPs and the Q_{abs} decrease	[37]

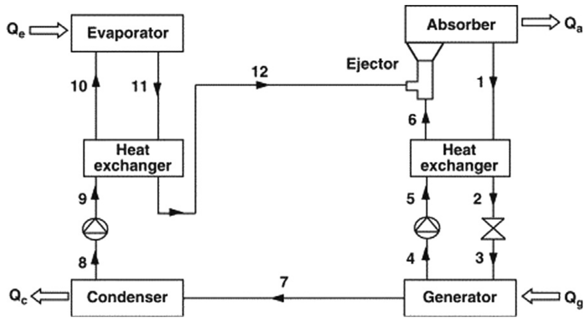


Fig. 6. Schematic representation of Ejector-Absorption Heat Transformer (EAHT) [24].

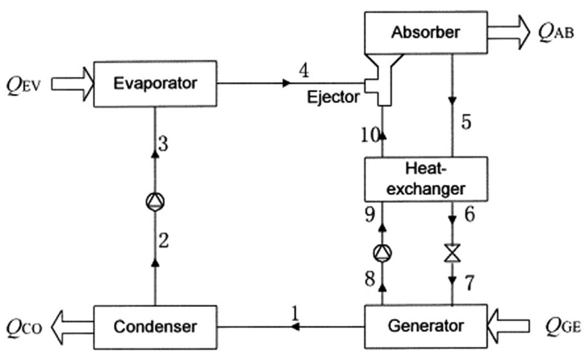


Fig. 7. Ejection–absorption heat transformer schematic diagram [26].

Shi et al. [26] presented and analyzed an ejection–absorption heat transformer (EAHT) based on the performance analysis of the single stage, the two-stage, and the double absorption heat transformers (Fig. 7).

Their results showed that it had a simpler configuration than the double absorption heat transformer and two-stage heat transformer. The delivered useful temperature in the ejection–absorption heat transformer was higher than that for a single stage heat transformer, and simultaneously, its system performance was increased.

Guo et al. [27] developed a mathematical model of a vertical falling film AHT with a water/lithium bromide solution to analyze the performance of AHTs under design and off-design conditions (Fig. 8). The study showed that the proportion of exergy losses in auxiliary components is small in design conditions, but increases rapidly in off-design conditions. Furthermore, a novel operation strategy based on keeping the circulation ratio invariant was proposed, leading to a significantly higher COP and exergy efficiency under off-design conditions.

Olarte-Cortes et al. [28] analyzed the heat transfer of an experimentally untested geometry in absorbers (Fig. 9) using tar impregnated graphite disk and LiBr/H_2O as working fluid. The impregnated tar was used to overcome the problem of corrosion faced by the conventionally used steel. Their results showed that as the Reynolds number increases from 110 to 144, the heat transfer coefficient increases, which lead to a maximum value of 954 W/m^2 K at Reynolds number of about 144, but when Reynolds number was increased above 147, the heat transfer coefficient decreased.

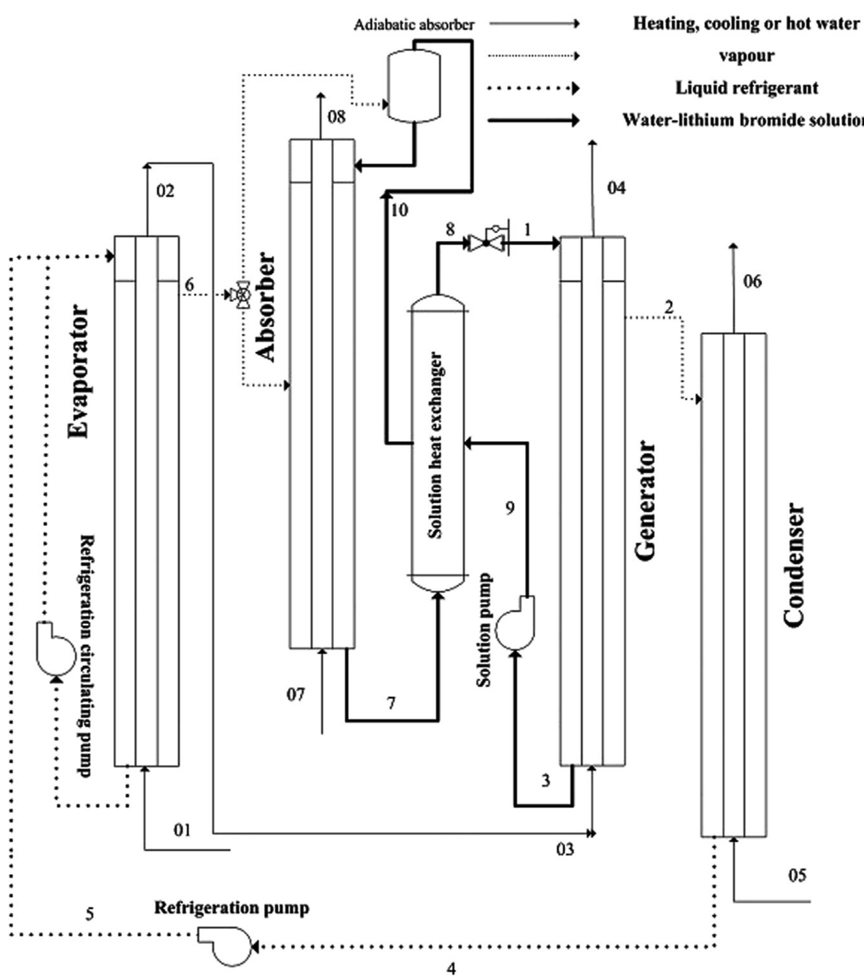


Fig. 8. Schematic diagram of the vertical falling film AHT [27].

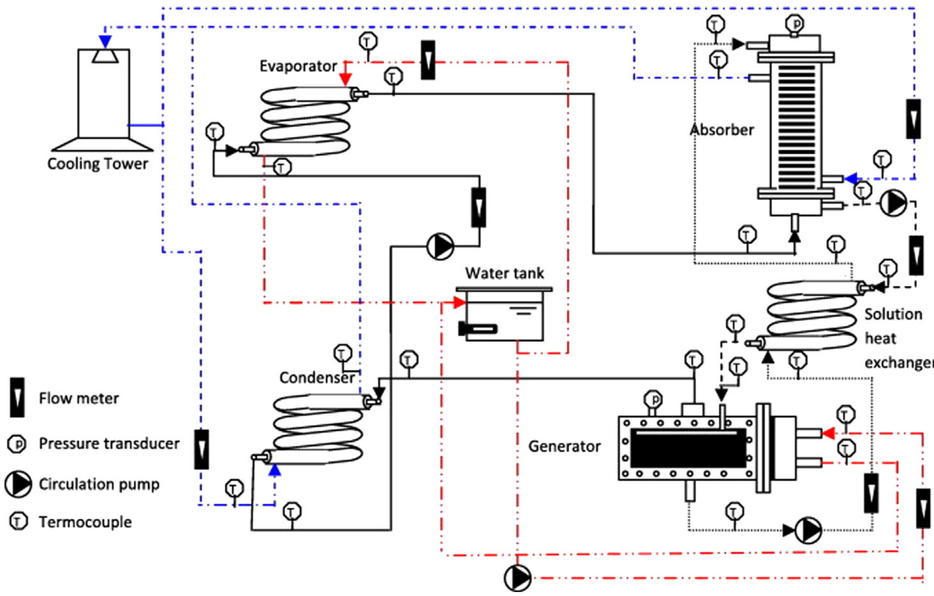


Fig. 9. Schematic diagram of the experimental bench using graphite disk [28].

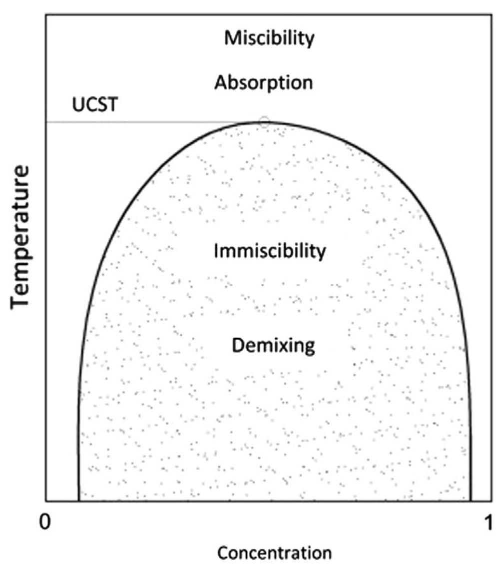


Fig. 10. Phase diagram of a partially miscible solution [29].

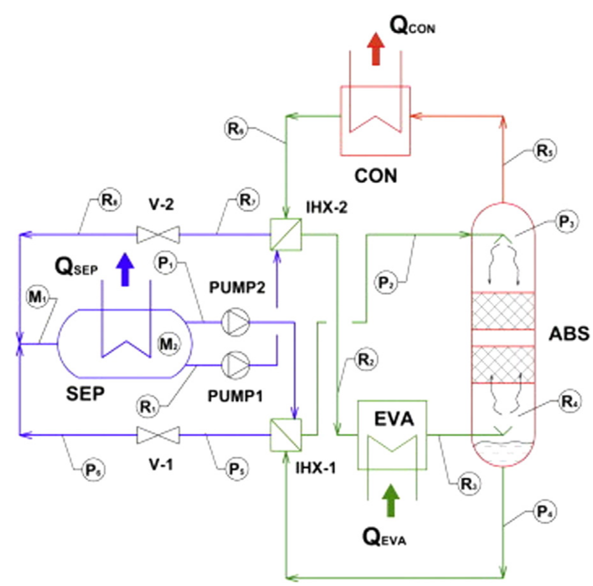


Fig. 11. Schematic diagram of the AHT-process using partially miscible working mixtures with upper critical solution temperature [29].

Absorption–demixtion heat transformer (ADHT) is a kind of absorption cycle which makes use of a mixture which exhibits a miscibility gap at low temperatures. The working mixtures used in this type of AHT process have an upper critical solution temperature (UCST) and consist of two components, one being much more volatile than the other. At temperatures higher than the UCST, the mixture is completely miscible. Below this temperature, it is partially miscible as shown in the phase diagram (Fig. 10). When utilizing this phenomenon in an AHT, absorption occurs at temperatures above the USCT, and demixing (desorption) at temperatures lower than the USCT.

Fig. 11 shows a schematic of an ADHT cycle. As the working pair enters the separator, it is demixed by rejecting heat to an external heat sink. Both mixtures are pumped separately to higher pressures and then heated in two internal heat exchangers. The refrigerant enters the evaporator, where it absorbs heat from an external source and vaporizes, then enters through the lower part of the absorber while the absorbent enters through the upper part. In the absorber, the concentration of the refrigerant decreases while its temperature increases. This results in the vapor mixture exiting at temperatures higher than the inlet temperature from the upper part of the absorber. The rest of the mixture exits from the lower part of the absorber where it is cooled in the internal heat exchanger and then throttled to a lower pressure before entering the separator.

The generated vapor mixture enters the condenser, and rejects heat at high temperature level to an external heat sink while it condenses. It is later cooled down in the internal heat exchanger and throttled to the low pressure level. Finally, the liquid mixture of the absorbent and refrigerant flows into the separator and mixes there with the rest of the mixture. The COP of ADHT-process is defined as follows [29]:

$$\mathrm{COP} = \frac{\text{condense capacity}}{\text{evaporator capacity}} \tag{1}$$

Liquid–liquid vapor equilibrium data was used by Niang et al. [30] to investigate an AHT process using a partially miscible working mixture of ($H_2O/(C_3H_3OC)CHO$) as an alternative to the

conventional H_2O/LiBr. In their work, a relatively higher COP of 0.86 was estimated. Alonso et al. [31] built the first experimental set-up of an ADHT to validate its technical feasibility using n-heptane/N,N-dimethylformamide (DMF) as working mixture. In the set-up used in this work, temperature lifts of maximum 80 °C and efficiencies of 0.3–0.4 were reported.

3. Double effect and double stage AHTs

Because the available temperature lift for single-stage absorption heat transformer (STAHT) is only in the range of 30–40 °C, it is expected that a better temperature lift must be obtained by adopting a two-stage absorption heat transformer (TSAHT) or a double absorption heat transformer (DAHT). Two-stage absorption heat transformer consists of two single-stage absorption heat transformers, so it has more components and more investment in equipment, while double-absorption heat transformer not only is an advanced absorption heat transformer in which it is possible to reach an absorbing temperature as high as that is reached by two-stage heat transformer, but also has the advantage of being considerably simpler than the two-stage heat transformer.

As shown in Figs. 12–14, only an absorbing evaporator and a pump must be added to a single-stage heat transformer to convert it into a double absorption heat transformer.

The performance of the DAHT shown in Fig. 12 has been presented by Rivera et al. [32,33]. However, this cycle had a drawback; the absorption or evaporation temperature in absorbing evaporator could not be as high as desired, since the weak solution leaving the absorbing evaporator absorbs vaporized water twice, and has the lowest concentration, such as $X_{AE} < X_{AB} < X_{GE}$.

A new solution cycle in the double absorption heat transformer (Fig. 13), which was an improved version of the earlier mentioned configuration, was proposed by Zhao et al. [34].

Because the vaporized water is absorbed only once, the concentration of the weak solution leaving the absorbing evaporator is higher than that in the cycle shown in Fig. 12.The results showed

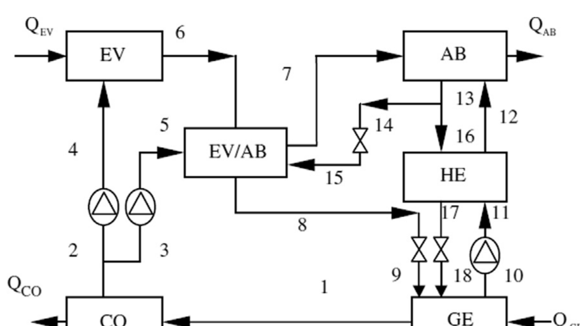


Fig. 12. Schematic diagram of DAHT (D-Type I) [32,33,35].

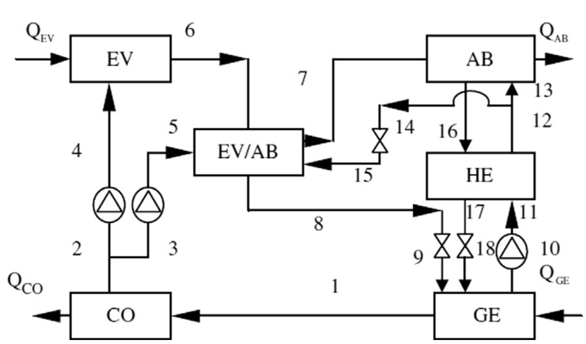


Fig. 13. Schematic diagram of DAHT (D-Type II) [34,35].

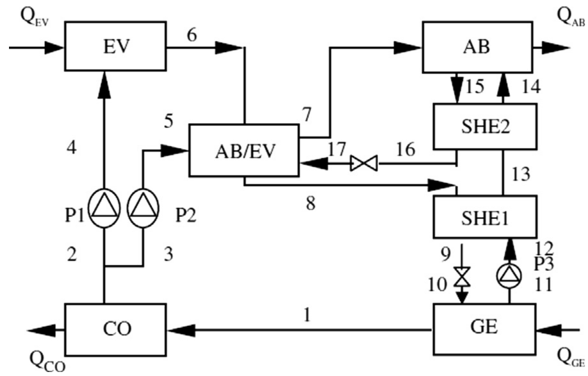


Fig. 14. Schematic diagram of DAHT (D-Type III) [35,36].

that this new cycle is superior to the cycle being studied by Rivera et al. [32,33]. This new solution cycle has a wider range of operation in which the system maintains the high value of COP and has larger temperature lifts and operation stability. The relationship between the absorber and the absorbing evaporator is more independent, and this makes the operation and control of the system easier. The weak solution leaving the absorber and that leaving the absorbing evaporator do not affect each other; consequently, a wider operating range of the new cycle will be possible.

Zhao et al. [35] studied thermodynamic performance of a new type of double absorption heat transformer (DAHT) (shown in Fig. 14) based on the thermodynamic properties of the aqueous solution of lithium bromide and the mass and energy balance for each component of the system. The solution cycle in the new type of DAHT was different from the ones mentioned earlier (shown in Figs. 12 and 13) [32–34,36], in which the temperature of the absorbing evaporator is not an independent variable, and the degree of freedom of the system is less than that of the DAHT with other solution cycles by one. (T_{AE} is a function of variables T_{GE} or T_{EV}, T_{AB} and T_{CO}). The results showed that, compared with other types of DAHT available in the literature, this new type of DAHT has a higher COP, especially when absorber temperature is higher. The COP could reach to a maximum value of 0.32, while maximum gross temperature lift could be in the region of 60–100 °C (shown in Table 2).

They found that T_{AE} increases with the increase of the T_{AB}, T_{CO}. Conversely, the effects of the condenser temperature on the temperature of the absorbing evaporator T_{AE} are less significant than those of the T_{AB} (D-Type I).

Configurations of double absorption heat transformers were also studied by Martinez and Rivera [37] from the viewpoint of the first and second laws of thermodynamics operating with the water–lithium bromide mixture.

Their results indicated that the generator had the highest irreversibility or exergy destruction contributing to about 40% of the total exergy destruction in the whole system. The results also showed that the COP and ECOP increase with increase in the generator, the evaporator, and the absorber–evaporator temperatures, and decrease with the absorber and condenser temperatures. Finally, it was observed that the COP and ECOP are very dependent on the FR and the economizer efficiency value.

Horuz and Kurt [5] simulated an industrial application of two different configurations of double absorption heat transformers (Types II and III) in a textile company for the aim of obtaining hot water, and compared them with single AHT. In their earlier mentioned work [8], they had proven that if the evaporator temperature is higher than the generator temperature, the AHT system performs better (COP and the absorber heat capacity increase). Hence, the waste hot water was first directed to the evaporator and then to the generator ($T_{gen} = T_{eva} - 10$ °C). Their

Table 2
Double stage absorption heat transformer.

Configuration	T_{eva} (°C)	T_{gen} (°C)	T_{con} (°C)	T_{abs} (°C)	T_{AE} (°c)	Working pair	f	GTL (°c)	COP	Heat Source	Remarks	Reference
D-Type I	70	70	20	130–170	70–130	H_2O–LiBr	$5 < F_{R1} < 65$ $2 < F_{R2} < 30$	60–100	0.25–0.31	-	* The absorption or evaporation temperature in absorbing evaporator cannot be as high as possible	[42,43,45]
D-Type II	70	70	20	130–170	70–130	H_2O–LiBr	$2 < F_{R1} < 60$ $2 < F_{R2} < 22$	5–10% higher than Type I	About 1% lower than Type I	-	*COP keeps a high value in a wider range of $T_{abs\text{-}eva}$ * A higher temperature in the absorbing evaporator can be obtained *Larger temperature lift (compared with type I)	[44,45]
D-Type III	70	70	20–35	120–195	87–127	H_2O–LiBr	-	60–100	0.316–0.32	-	Higher COP compared with previous types of DAHT(Type I, Type II), especially when more large temperature lift is needed	[45,46]
D-Type I	75–90	75–90	30–40	140–165	100–115	H_2O–LiBr	5–29		0.12–0.32	-	FR should be as low as possible in order to increase significantly the ECOP and the exergy COP values of the system.	[47]
D-Type II	80	70	25	160	115	H_2O–LiBr	-	80	0.377	Waste heat from a cogeneration system in a textile company	*Higher heat transfer in absorber compared with Type III	[15]
D-Type III	80	70	25	160	115	H_2O–LiBr	-	70–80	0.405	Waste heat from a cogeneration system in a textile company	*Higher COP than Type II	[15]
DEAHT	$T_{HG}-3$	$90 < T_{HG} < 110$	30	90–155	-	H_2O–LiBr	-	-	0.58–0.65	-	The range of GTL of DEAHT is narrower than that of the SAHT	[50]
DEAHT	$T_{HG}-3$	$90 < T_{HG} < 110$	30	90–155	-	TFE/E181	5–40	-	0.48–0.62	-	Acceptable magnitudes of COP	[50]
DSAHT	$T_{eva1}=53.9$ $T_{eva2}=72.3$	50.6	22.2	$T_{able1}=77.2$ $T_{able2}=101.8$	-	H_2O–LiBr	-	-	0.37	-	Generator has the largest exergy loss	[51]

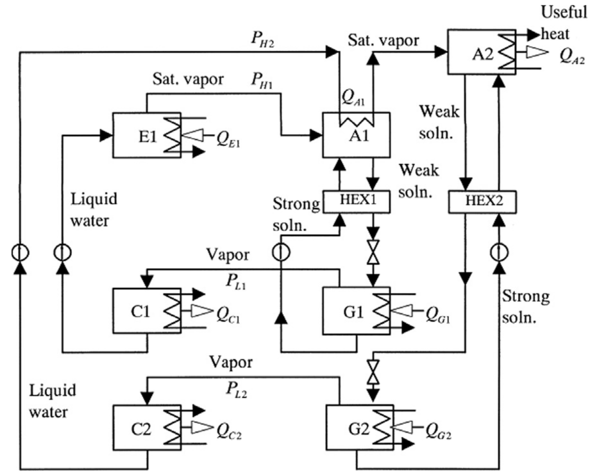


Fig. 15. Basic two-stage absorption heat transformer [38].

analysis provided evidence that the Type II double AHT system had lower COP than Type III, but it could generate more water vapor.

Ji and Ishida employed Energy-Utilization Diagrams (EUDs) for investigating a two-stage absorption heat transformer and its improved versions [38]. In the first case, they studied a basic two-stage absorption heat transformer (Fig. 15).

Then, in the second and third cases, they applied close-to-equilibrium operation to generators (multiple-compartment generator) and absorbers (multiple-compartment absorber) (Fig. 16).

Through this study, it has been concluded that by modifying the two-stage absorption heat transformers, higher performances can be achieved, and the exergy efficiencies can be increased from 48.14% to 54.95%.

Shiming et al. [39] proposed an alternative system known as a self-regenerated absorption heat transformer (SRAHT), which utilizes a new organic working pair (TFE-NMP). Fig. 17 shows a schematic of this system [39].

The new working pair had some advantages compared with H_2O–LiBr and NH_3–H_2O, including, wide working range as a result of the absence of crystallization, low working pressure, low freezing temperature of the refrigerant, and good thermal stability of the mixture at high temperatures. On the other hand, it had lower boiling temperature difference between TFE and NMP, which is a negative feature (similar to NH_3–H_2O a rectifier was needed). They found out that SRAHT could recover more waste heat and had a larger temperature lift compared with the conventional AHT cycle using H_2O–LiBr, although its COP was lower.

Zhao et al. [40] developed a code for a double effect absorption heat transformer (Fig. 18) and used Trifluoroethanol (TFE)–tetra-ethylenglycoldimethylether (TEGDME or E181) as a new organic working-pair which was non-corrosive, completely miscible, and thermally stable up to 250 °C. The results showed that, when the temperature in the high-pressure generator exceeded 100 °C, and the gross temperature lift was 30 °C, the COP of the DEAHT was about 0.58, which was larger than the 0.48 of the single-stage absorption heat-transformer (SAHT); consequently, the increase of COP was about 20%. But it was still less than 0.64 of the DEAHT using LiBr–H_2O as the working fluid.

Farataj performed energy, exergy, and entropy balance analyses for a double-stage, LiBr–water absorption heat transformer cycle [41] (Fig. 19).

In the particular case considered, the largest exergy loss within the system resulted in the generator, indicating that efforts should be focused on improving this component.

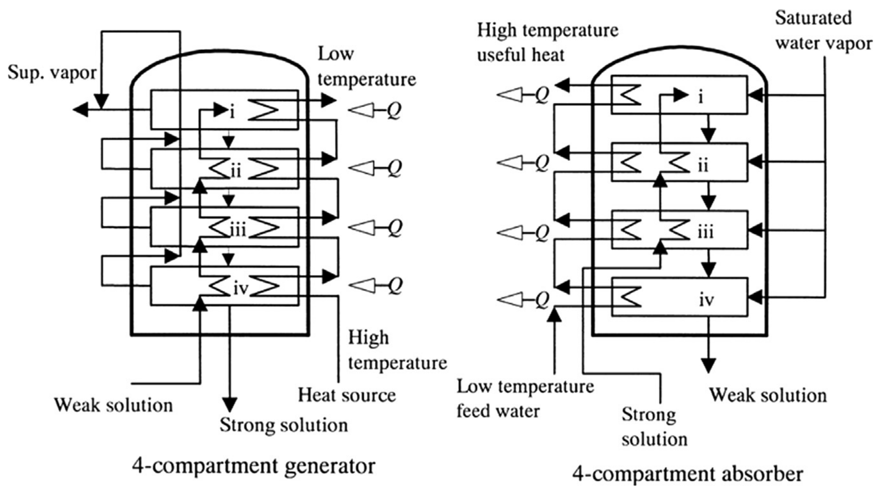


Fig. 16. The generator and absorber in close-to-equilibrium operation [38].

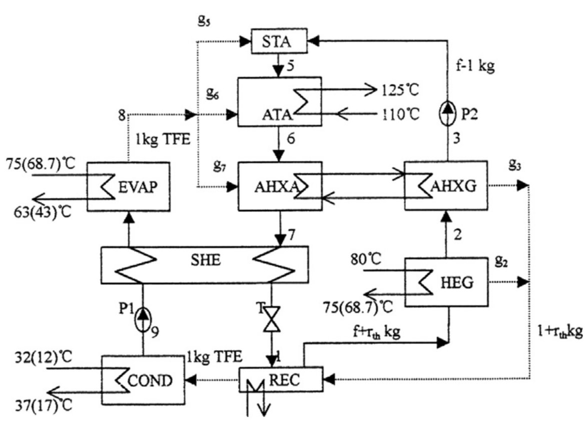


Fig. 17. Self-regenerated absorption heat transformer (SRAHT) cycle flow diagram [39].

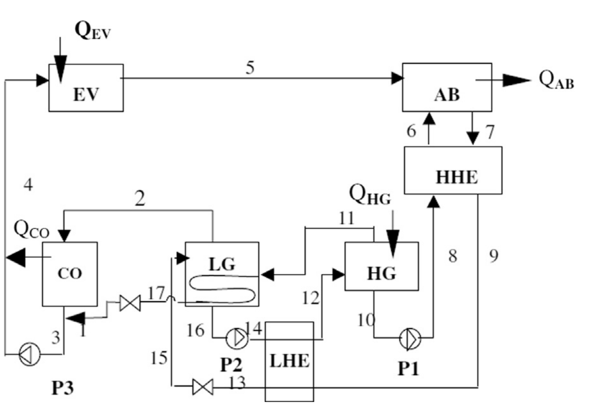


Fig. 18. Configuration of a double-effect absorption heat-transformer [40].

Very recently, Donnellan et al. [4] dissected and reassembled the design of a triple absorption heat transformer (TAHT) utilizing H_2O/LiBr as the working pair, and using heat exchange network modeling in order to determine the optimum number and locations of internal heat exchange units within the system (Fig. 20). They found out that the conventional design of the TAHT does not employ heat exchangers effectively, and that thus by rearranging these units, COP may be increased by 11.7% while exergy destruction within the system could be reduced by 21%. Strategically adding an extra one or two heat exchangers increased the COP by 16.4% and 18.8%, while decreasing exergy destruction by 28% and 31.5%, respectively.

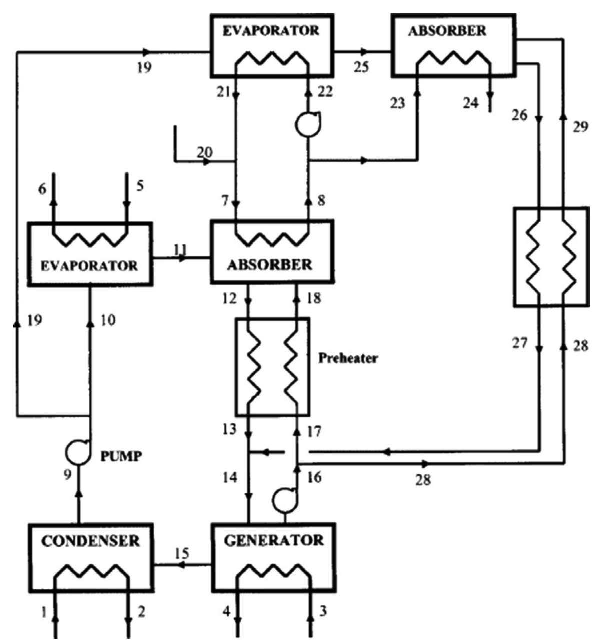


Fig. 19. Schematic of double-stage heat transformer [41].

- All temperatures are in degree Celsius.
- In the cases which temperatures of generator and evaporator are not equal we have considered GTL$=T_{abs}-T_{max}$ (higher temperature between T_{gen} and T_{eva}).

3.1. An overall comparison among typical configurations of AHTs

Three main types of typical AHTs including single, double and triple systems, using LiBr/H_2O as the working fluid, are analyzed thermodynamically by the authors. The waste heat from a textile factory is utilized to run the AHT [8]. A computer program is developed in Engineering Equation Solver (EES) to investigate the effects of different parameters on different categories of AHT.

The considered assumptions for all the configurations are the same with the ones previously published in Refs. [4,37,42] which are used for single, double and triple AHTs, respectively.

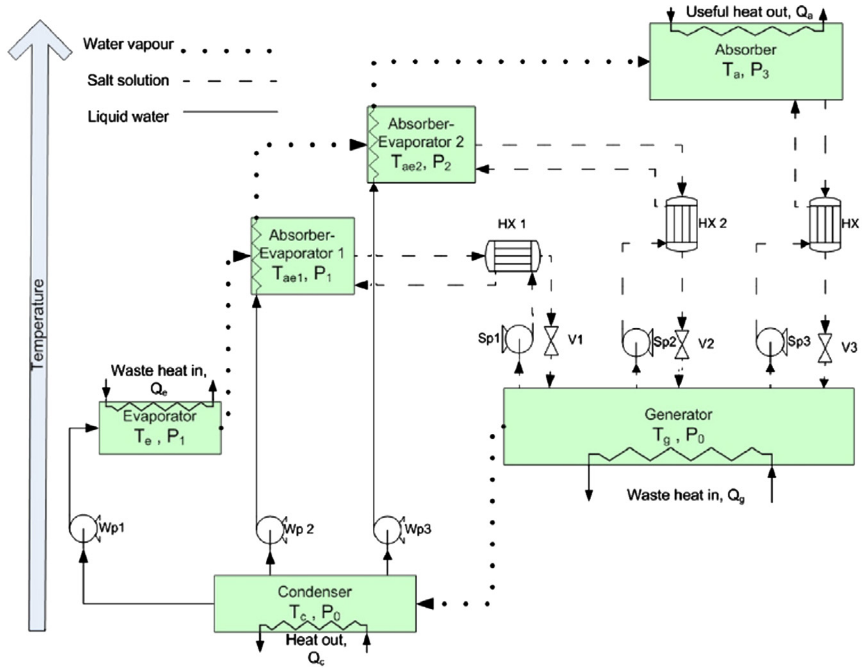


Fig. 20. Schematic of the conventional triple absorption heat transformer (TAHT) (redrawn by authors) [4].

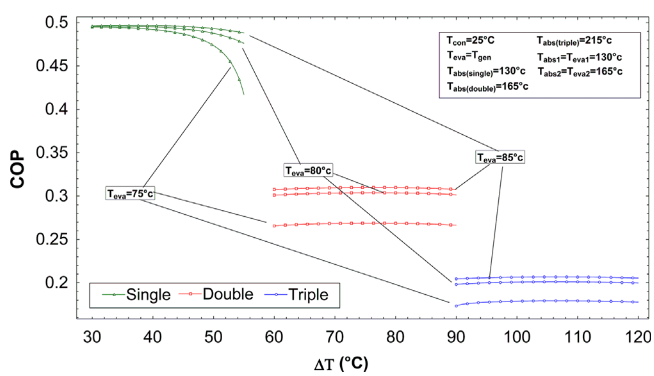


Fig. 21. Effects of T_{abs} on COP for different types of AHTs at different evaporation temperatures.

The available data in the literature were used to validate the simulation results [Rivera]. For the case of the single stage AHT cycle the experimental results reported by Rivera et al. [43] are used. The conditions and assumptions used in their work are applied for the aim of validation.

Fig. 21 shows the variation of COP with the absorption temperature under different evaporation temperature conditions. As can be seen, any increase in absorber temperature will cause a drop in the COP. This is due to the fact that as T_{abs} increases, the concentration of the weak solution and consequently the flow ratio (f) increase, resulting in a decrease in the absorber heat capacity. This result is in agreement with that reported in the literature [8,42].

As shown in Fig. 21 the higher the evaporation temperature is, the higher the absorption temperature and the corresponding gross temperature. It is observed that SAHT has the highest COP and the TAHT has the lowest. The same trend has been reported by Donnellan et al. [4].

4. Applications of AHTs

A single effect AHT using H_2O–LiBr was employed by Yari [44] in a novel cogeneration cycle (CC) where the recompression of S–CO_2 in a Brayton cycle that utilized the waste heat from a nuclear power plant was proposed (Fig. 22). It was found that both the energy and exergy efficiencies of the new S–CO_2 cycle were higher than that of the simple S–CO_2 cycle by 5.5–26%. A maximum pure water flow rate of 3.317 kg/s was obtained under the analyzed condition for the new S–CO_2 cycle. The exergy destruction value of the new cycle was on average 12.6–19.1% lower than that of the conventional cycle (without AHT and desalination system).

Zare et al. [45] utilized the waste heat from a gas turbine-modular helium reactor (GT-MHR) to produce power through two Organic Rankine Cycles (ORCs) and pure water by means of distillation processes (Fig. 23). A single stage absorption heat transformer (AHT) was employed to upgrade the lower temperature waste heat in order to run the desalination system. The proposed cycle performance was then optimized based on the first law of thermodynamics. The results showed that the first law efficiency of the CC cycle, at the optimum conditions, is around 7% higher than that of the GT-MHR cycle. It was also concluded that for each 50 °C increase in the gas turbine inlet temperature, the thermal efficiency is increased by around 2.5–4% and the pure water production rate is decreased by around 6.5%.

In another work Yari et al. [46] proposed and analyzed a combined cogeneration cycle (shown in Fig. 24) in which the waste heat from an ejector-expansion trans-critical CO_2 refrigeration cycle was utilized for power production and water purification simultaneously. The waste heat utilization was performed by means of a CO_2 supercritical power cycle and a desalination system for pure water production. In order to run the desalination system, a single stage absorption heat transformer was employed to upgrade the lower temperature waste heat. It was found that, at the optimum conditions, the energy efficiency ratio of combined cogeneration cycle was about 13–45% higher than the coefficient of performance of the ejector-expansion trans-critical CO_2 cycle (without AHT and desalination system).

Huicochea et al. [47] studied the potential of a novel cogeneration system which consisted of a 5 kW proton exchange membrane fuel cell (PEMFC) and a single stage absorption heat transformer. The dissipation heat resulting from the operation of the PEMFC would be supplied to the absorption heat transformer,

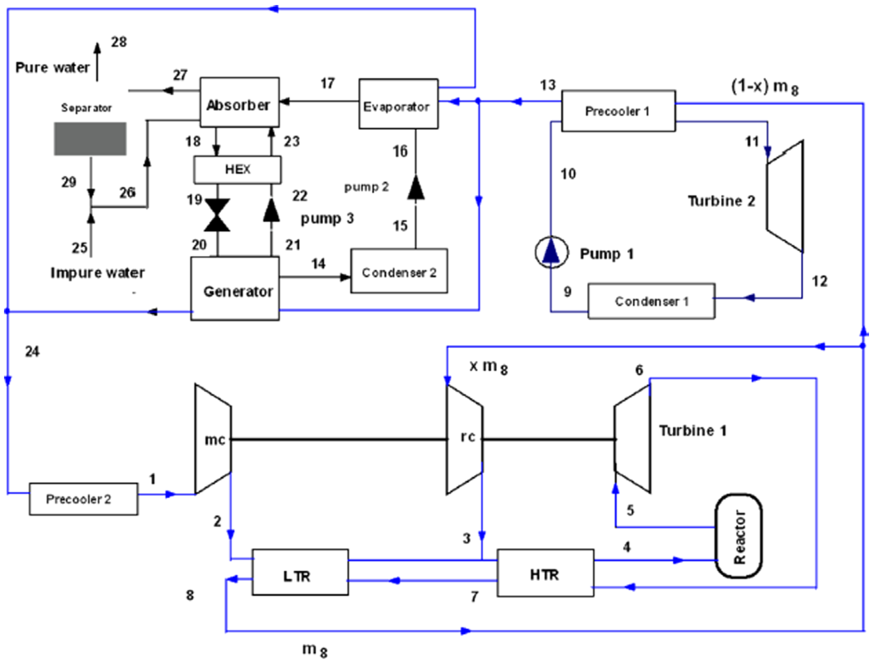


Fig. 22. Schematic of the new recompression S–CO_2 cogeneration cycle [44].

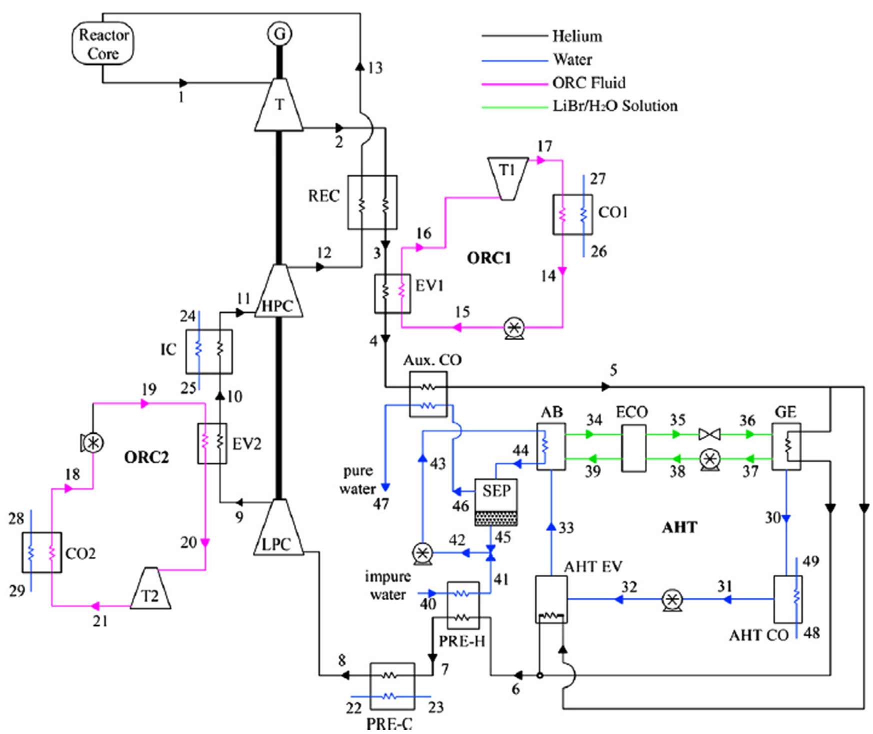


Fig. 23. Schematic diagram of the CC cycle [45].

which was integrated to a water purification system. Therefore, the products of the proposed cogeneration system were heat, electricity, and distilled water as seen in Fig. 25. The study performed a simulation for the PEMFC and used results obtained from an experimental AHT facility. The results showed that experimental values of coefficient of performance of the AHT and the overall cogeneration efficiency could reach up to 0.256 and 0.571, respectively. A 12.4% efficiency improvement was obtained, compared to the fuel cell efficiency working individually. The study showed that the combined use of AHT systems with a PEMFC was a feasible project.

Sekar and Saravanan [48] coupled a single effect AHT with MultiEffect Desalination (MED) systems for the purpose of water purification (Fig. 26). They made an exergetic analysis and evaluated the exergetic efficiency, exergy losses in the components, and exergy balance of the system. The effects of operating parameters such as the temperatures of the heat source, sink temperature, and the effectiveness of the solution heat exchanger were evaluated on the performance of the system. Exergy efficiency varied from 11.14% to 35.35% depending on the temperatures of heat source and sink. It was found that the highest exergy loss was in the condenser of AHT, followed by the second effect of

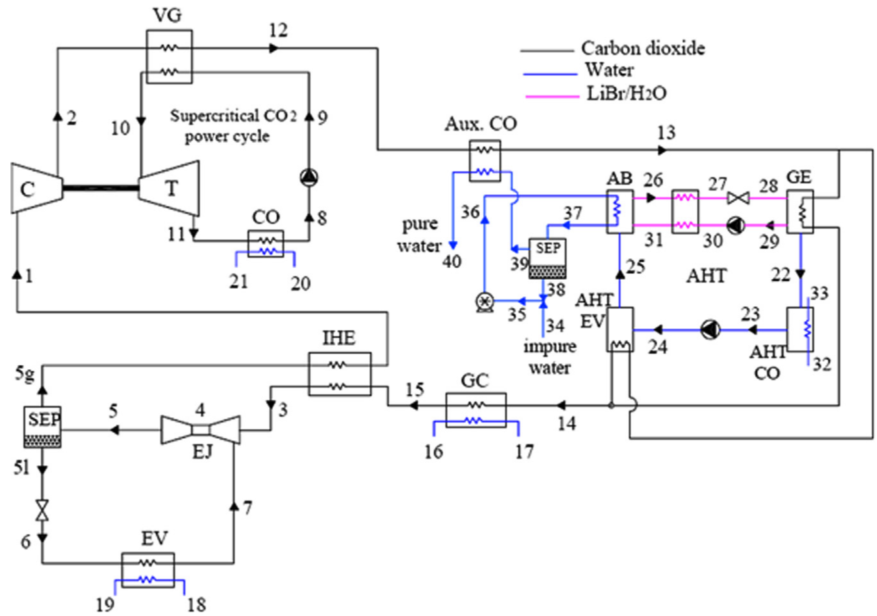


Fig. 24. Schematic diagram of the combined cogeneration cycle [46].

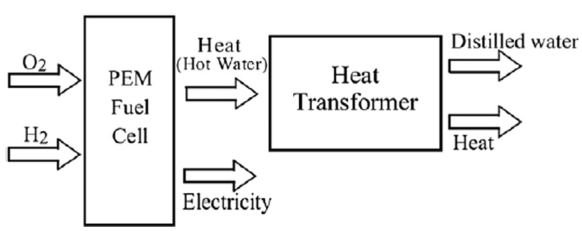


Fig. 25. Schematic diagram of the cogeneration system formed by a proton exchange membrane fuel cell and an absorption heat transformer [47].

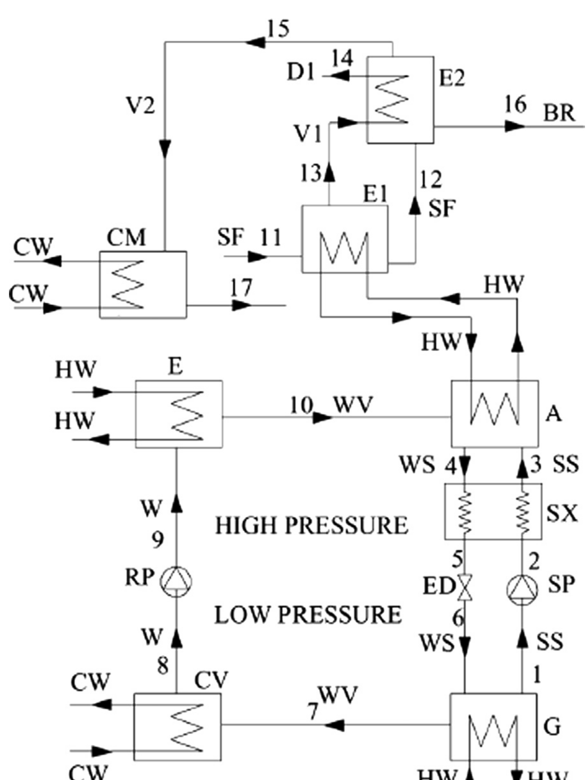


Fig. 26. Schematic diagram of AHT coupled with multi-effect desalination [48].

the MED system. They reported that increasing the gross temperature lift increases the exergetic efficiency and effectiveness of the solution heat exchanger, and decreases the exergy losses.

Gomri modeled the single and double effect absorption heat transformer systems used for seawater desalination [49] (Fig. 27a and b). The results obtained from his study showed that the energy and the exergy efficiencies of the double effect absorption heat transformer are higher than those of the single effect absorption heat transformer. However, on the other hand, water production is slightly higher for the single effect absorption heat transformer integrated to a desalination system than that for double effect absorption heat transformer.

In another work, Gomri presented the installation and use of a flat plate solar collector (FPC) to a single effect AHT with a desalination system [50] (Fig. 28). The energy and exergy analyses were carried out for each component of the system on 21 July 2009, in Skikda (East of Algeria; Latitude 36.52°N, Longitude 6.57°E), between 8 am and 4 pm. Considering all the components in the desalination plant, Gomri concluded that the highest exergy destruction was generated in FPC.

A feasibility study of the implementation of a double lift heat transformer in a Kraft pulping process was performed by Costa et al. [51]. They integrated a double lift heat transformer into the heat recovery circuit of the woodchips digesters to produce low-pressure steam equivalent to 25%. They concluded that a double lift AHT working with the H_2O/LiBr pair could be driven by the contaminated steam coming out from a blow tank with a COP of 0.35 and produce17 t/h of low pressure steam (Fig. 29).

In another work, Ji and Ishida [52] assessed an exergy analysis based on the energy-utilization diagram (EUD), applied to humid air turbine cycle, incorporated with a modified two-stage absorption heat transformer as mentioned in Ref. [38] (Fig. 30).

Employing the sensible and latent heat exchange modes in the modified two-stage absorption heat transformer in supplying heat to the humid air turbine cycle clarified that this method could intensively recover the waste heat of humid air turbine cycle and improve system performance. Compared to a conventional HAT cycle, the overall cycle efficiency and the specific work were increased by 2% and 7%, respectively.

Huicochea et al. [53] integrated experimentally a single effect absorption heat transformer to a water purification system

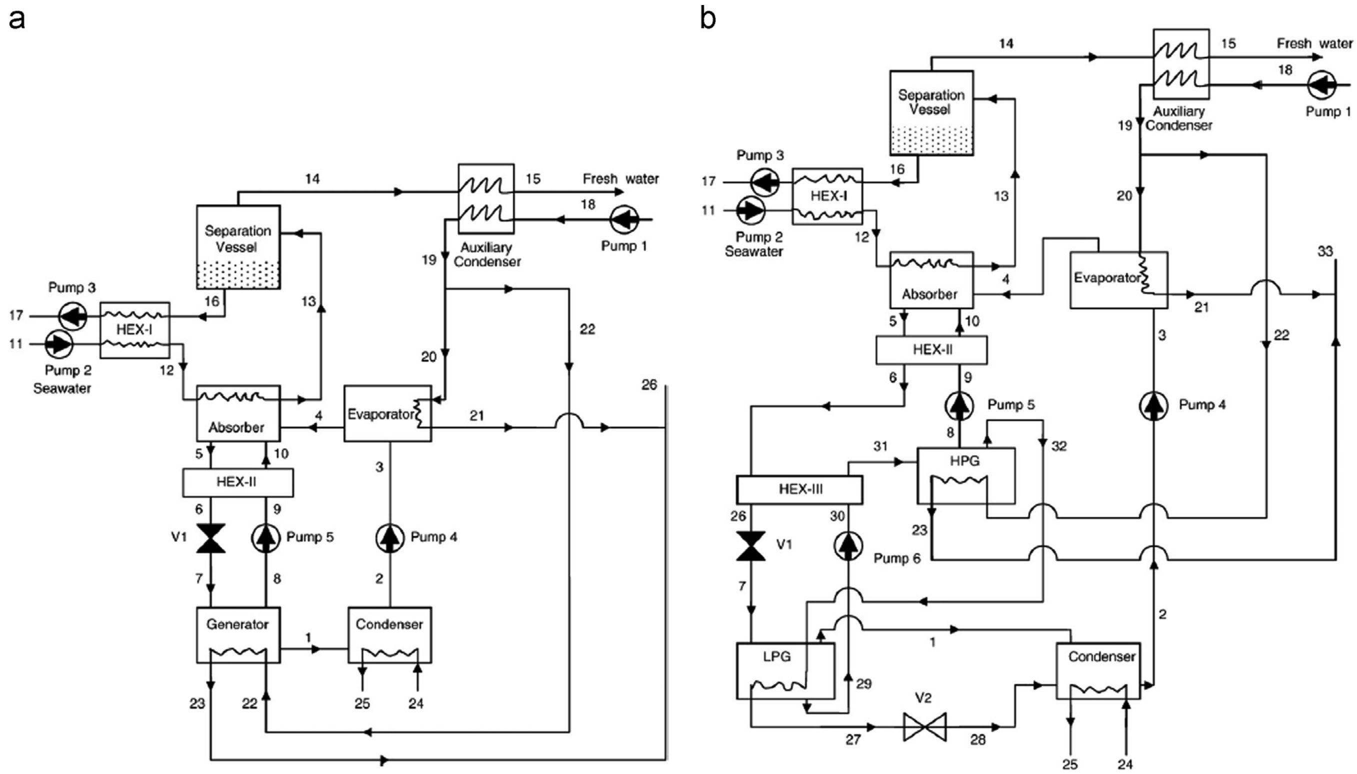


Fig. 27. (a) Schematic diagram of water purification integrated to a single effect absorption heat transformer [49]. (b) Schematic diagram of water purification integrated to a double effect absorption heat transformer [49].

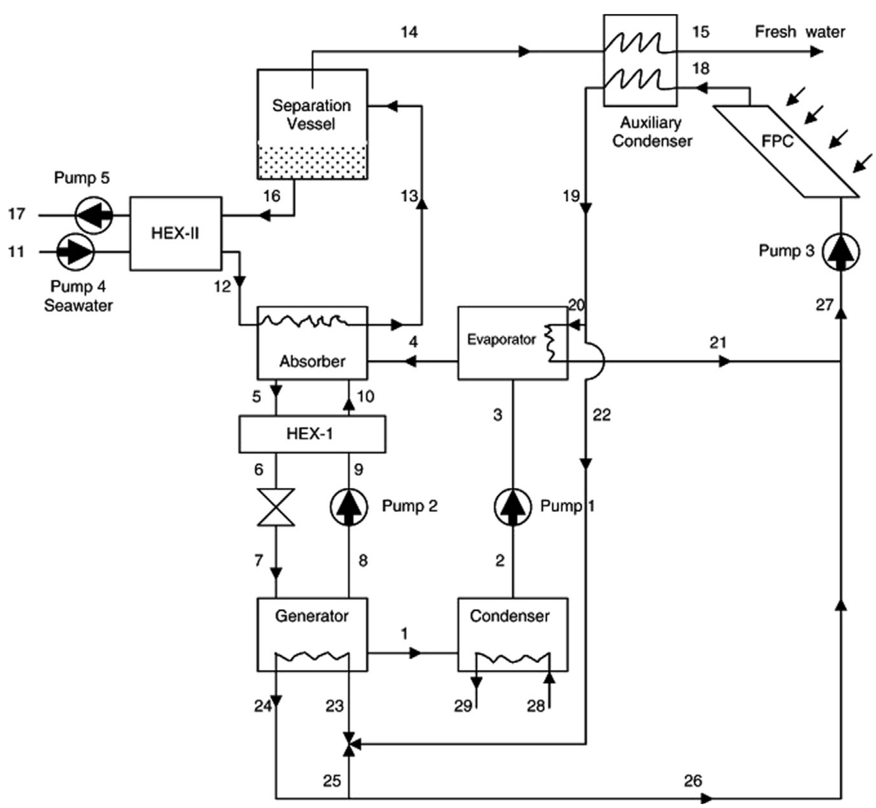


Fig. 28. Schematic diagram of water purification integrated to a solar heat transformer [50].

utilizing waste heat in the temperature range of 68–78 °C, with the consideration of recycling the fraction heat obtained from auxiliary condenser, in order to increase the heat source temperature (Fig. 31).

They showed that COP_{AHT} and COP_{WP} increase when the concentration of the solution in the absorber becomes stronger. Similarly as COP rises, distilled water production increases too. Romero and Martinez [54] studied theoretically the same water

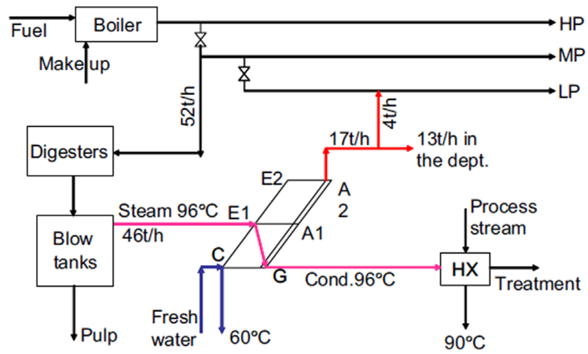


Fig. 29. Installation of a double lift AHT in the blow tank heat recovery circuit [51].

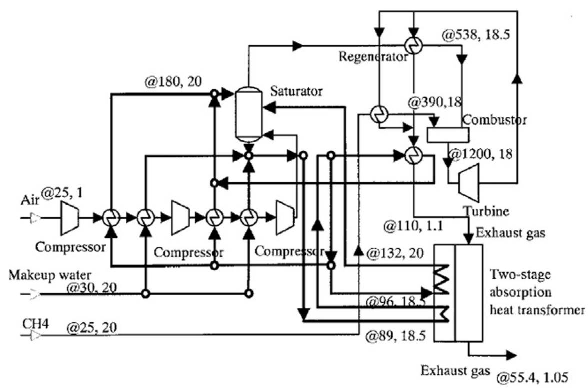


Fig. 30. A process flow for the humid air turbine cycle combined with modified two-stage absorption heat transformer [52].

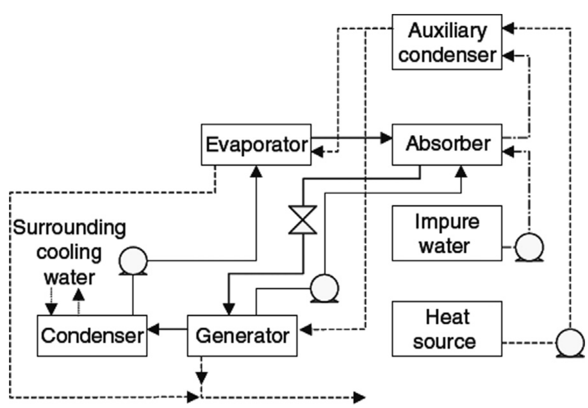


Fig. 31. Schematic diagram of water purification integrated to a heat transformer [53].

purification system. The results showed that the recycled energy had useful effect in COP, as it would increase from 0.3 to 0.429. Once again, Siqueiros and Romero [55] discussed the mentioned desalination system. The results demonstrated that the system was capable of increasing the COP more than 120% by recycling the energy obtained from the water purification system. Romero et al. [56] concluded in their second study that the AHTWP system was capable of increasing the original value of COP up to 1.6 times its original value by recycling energy from a water purification system.

The potential of using the fluid mixture water–(LiBr+LiI+$LiNO_3$+LiCl) was studied numerically by Bourouis et al. [57] for purification of seawater using single-stage absorption heat transformer (same as Fig. 31). The multi-component salt mixture showed a considerably higher solubility than that of the conventional working fluid water–LiBr. It is also less corrosive and has

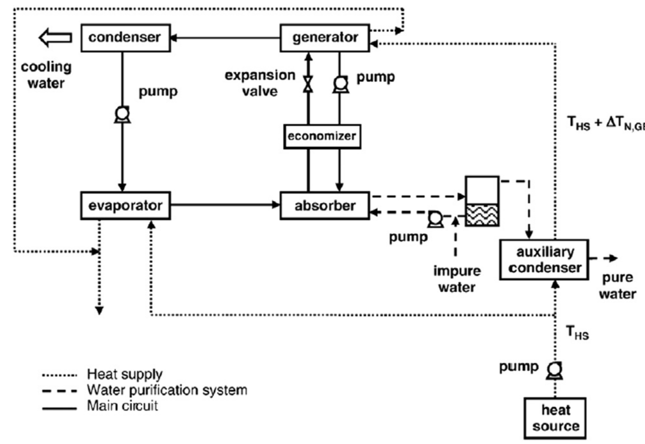


Fig. 32. Heat recycling applied to generator [58].

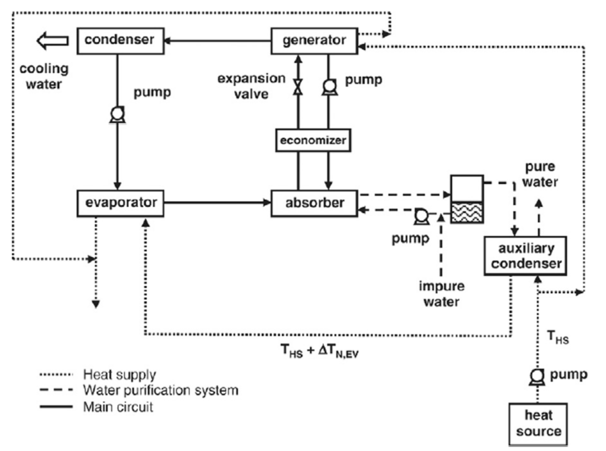


Fig. 33. Heat recycling applied to evaporator [58].

lower crystallization temperature than that of the LiBr solution. The integrated absorption heat transformer water purification system using the working fluid water–(LiBr/LiI/$LiNO_3$/LiCl) displayed better performance compared to the system using water–LiBr. The COP was higher and remained almost constant as the condensation temperature increased at the considered thermal operating conditions of the cycle. The wider range of solubility of the multi-component salt solution made possible the operation of the heat transformer cycle at higher concentrations of the strong solution.

Huicochea and Siqueiros [58] investigated 3 different configurations (Figs. 32–34) of water purification through single-effect evaporation, using H_2O/LiBr at 700 W thermal load. By applying heat recycling to either the evaporator, or the generator, or both, under the same performance conditions, they reported a considerable increase in the performance: 110.3%, 61.5%, and 79.3%, respectively.

Huicochae et al. [59] experimentally evaluated an absorption heat transformer coupled to a water purification system using a thermal bath to supply heat to the generator and evaporator, with a variable electric coil as shown in Fig. 34. They found that the system irreversibilities increase the COP, and the ECOP decrease with an increment of the mass flow of hot water supplied to the generator.

Sekar and Saravanan [60] conducted experiments on a vapor absorption heat transformer driven distillation system (Fig. 35) of 5 kg/h capacity, using water lithium bromide. They reported a COP between 0.30 and 0.38, and gross temperature lift varying between 15 and 20 °C.

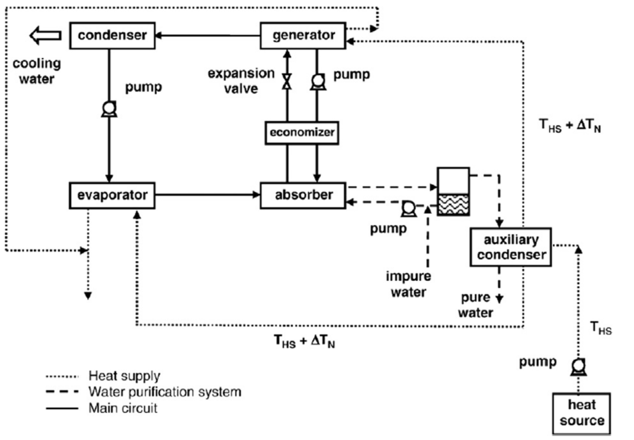


Fig. 34. Heat recycling applied to generator and evaporator [58].

Based on China's 600 MW existing coal-fired power plant, Duan et al. [61] investigated a Monoethanolamine (MEA) based CO_2 capture system. A Post Combustion Carbon Capture and Storage (PC+CCS), coupled with AHT and AHP (Fig. 36), was used to fully utilize the heat at low level. This recovered and upgraded heat was used for amine based solvent regeneration, leading to a noticeable decline in required energy.

Thermally activated systems based on sorption cycles, as well as mechanical systems based on vapor compression/expansion, were assessed by Little A. & S. and Garimella [62] for waste heat recovery applications. This study investigated four cases: waste heat recovery for data centers, vehicles, and process plants, illustrating the utility and limitations of such solutions.

In another application, Little and Garimella [63] conceptualized and analyzed a novel paradigm consisting of integrated power, cooling, with waste heat recovery, and upgrade systems that considerably lower the energy footprint of data centers. This system

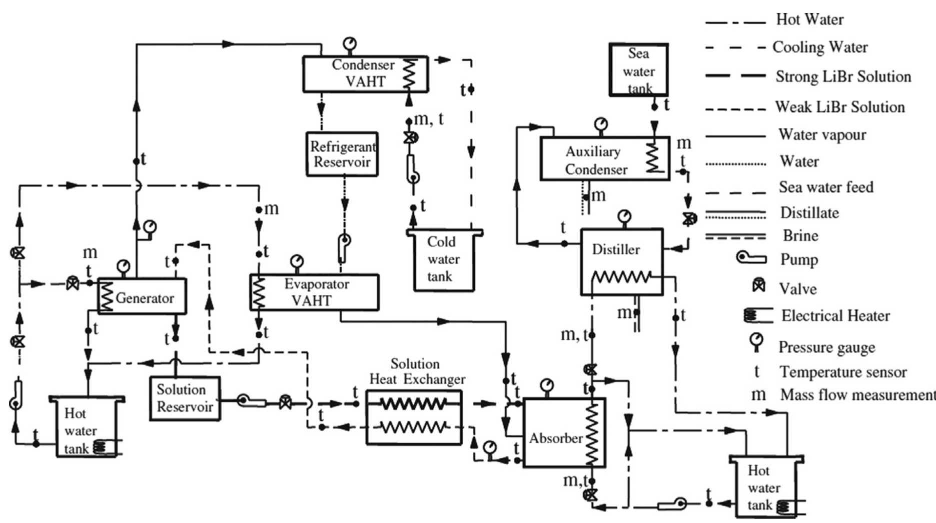


Fig. 35. Schematic of the experimental set-up [60].

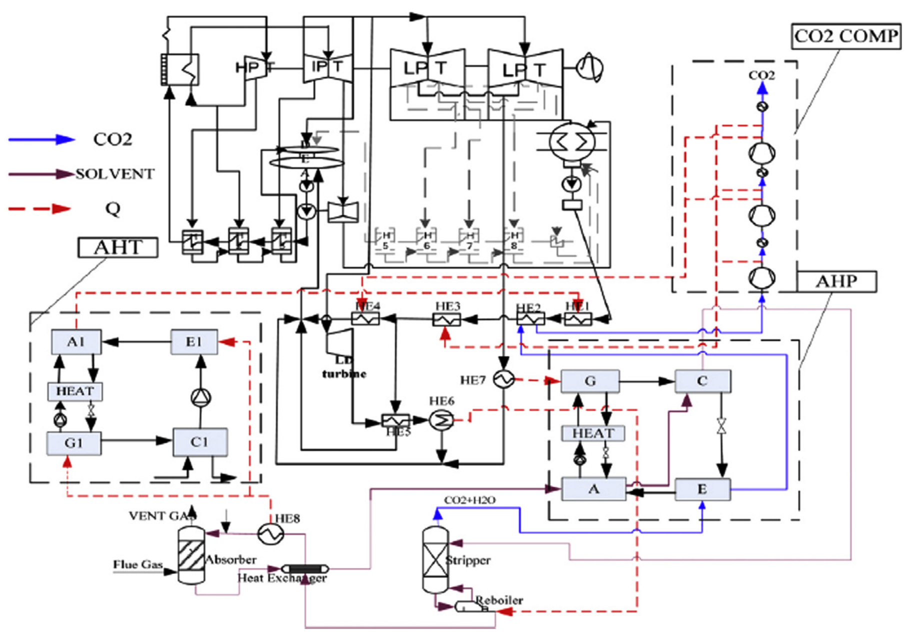


Fig. 36. Steam water schematic of (PC+CCS+AHT/AHP) [61].

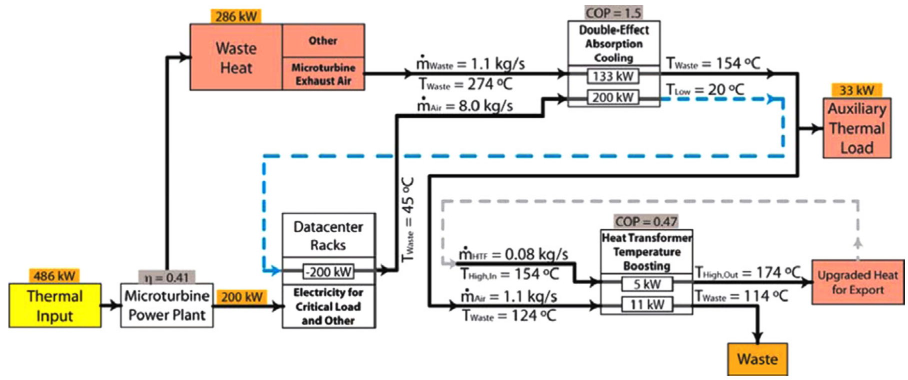


Fig. 37. Type 1 – Waste heat from micro-turbine exhaust air provides cooling to the data center operating in a closed air loop configuration. Rack air inlet and outlet temperatures are 20 and 45 °C, respectively, and 5 kW of upgraded heat at 174 °C is realized at the heat transformer [63].

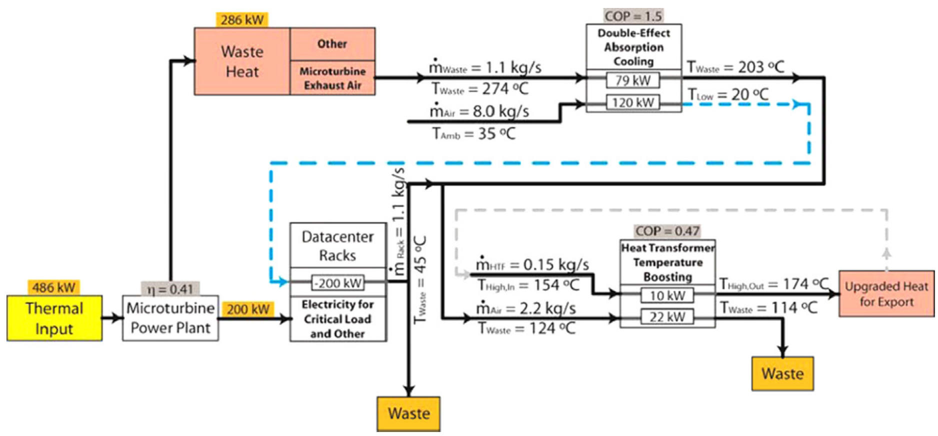


Fig. 38. Type 2 – Waste heat from micro-turbine exhaust air provides cooling to the data center and then is mixed with a portion of data center rack air exhaust to provide 10 kW of upgraded heat at 174 °C [63].

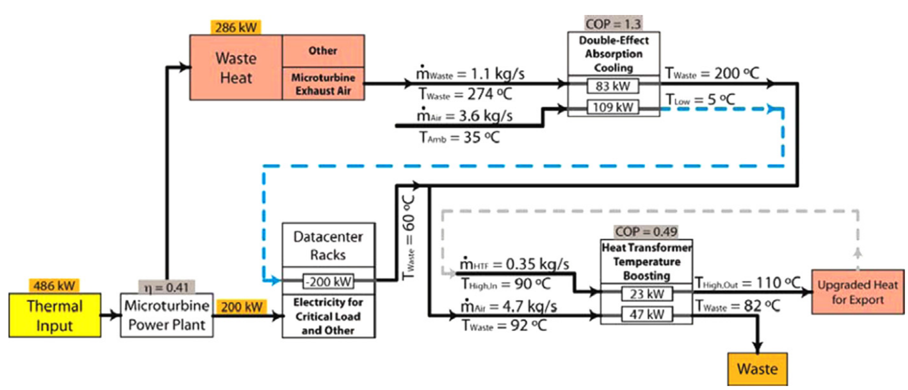


Fig. 39. Type3 – Waste heat from micro-turbine exhaust air provides cooling to the data center and then is mixed with all data center rack air exhaust to provide 23 kW of upgraded heat at 110 °C [63].

draws waste heat from an on-site micro-turbine power plant to provide the necessary cooling for the data center critical load, with a double-effect absorption chiller. The system was analyzed under various configurations as shown in Figs. 37–39. The performance and temperature lift of the AHT system are given in Table 3. An overall efficiency of 41% without the heat transformer was reported, and ranged from 42% to 46% when the heat transformer was added.

5. Working fluids

Barragán Reyes et al. [64] made a theoretical investigation on the performances of absorption heat transformers using $H_2O/CaCl_2$ and $H_2O/LiCl$ as working fluids. The results revealed better performance of $H_2O/LiCl$ compared to the $H_2O/CaCl_2$ in single stage absorption heat transformers.

Parham et al. [42] investigated thermodynamic performance of an absorption cycle using (H2O+LiCl) as the working pair by simulating and comparing by the cycle using (H2O+LiBr). The effects of evaporation temperature on the performance coefficient, COP, generation temperature, concentration of strong solution, and flow rate ratio were also analyzed. The results showed that the coefficient of performance of the cycle, using (H2O+LiBr) at the optimum conditions, was around 1.5–2% higher than that of (H2O+LiCl). On the other hand the crystallization problem had been resolved.

Table 3
Applications of absorption heat transformers.

Configuration	T_{eva} (°C)	T_{gen} (°C)	T_{con} (°C)	T_{abs} (°C)	Working pair	f	GTL (°C)	COP	Heat source	Remarks	Reference
Fig. 21	(75–80)-8°c	(75–80)-8°c	20	105–120	H_2O/LiBr	-	22–32	-	Waste heat from a nuclear power plant	*Increase in the energy and exergy efficiencies of the cycle	[52]
Fig. 22	63–75	63–75	20	105–115	H_2O/LiBr	-	47–59	0.44–0.51	Waste heat from a (GT-MHR)	*Increase in the first law efficiency of the CC cycle	[53]
Fig. 23	62–72	62–72	20	105–120	H_2O/LiBr	-	45–48	0.484–0.508	Ejector-expansion trans-critical CO_2 refrigeration cycle	* The COP and EER of both cycles are increased	[54]
Fig. 24	84–89	84–89	-	-	H_2O/LiBr	–	–	0.18–0.27	Waste heat from a proton exchange membrane fuel cell (PEMFC)	An increment of around 12.4% in the efficiency of cogeneration	[55]
Fig. 25	60–75	60–75	15–30	-	H_2O/LiBr	–	10–30	0.444–0.498	–	*Heat source temperature and sink temperature have considerable impact on the exergetic efficiency.	[56]
Fig. 26a	74–96	0.74–96	29	103–127	H_2O/LiBr	–	29–31	–	–	Slightly higher water production than that for double effect absorption heat transformer	[57]
Fig. 26b	87–96	87–96	29	103–155	H_2O/LiBr	–	16–59	–	–	Higher energy and the exergy efficiency than that of the single effect absorption heat transformer	[57]
Fig. 27	T_{out}-3 (T_{out} is the outlet temperature of Collector after heat exchanger)	T_{out}-3	29	103	H_2O/LiBr	–	–	≈ 0.5	–	The energy efficiency of WP is higher than that for FPC and AHT.	[58]
Fig. 30	62.5–72.5	70.7–75.8	31.7–34	96.3–98.4	H_2O/LiBr	–	22.6–25.6	0.09–0.228	–	The distilled water quality is similar to that obtained from a laboratory's electrical distiller.	[61]
Same as Fig. 30	60–75	60–80	25–30	105–115	Not mentioned			1.2–5	Industrial waste heat	The recycled energy for latent heat of purified water purification system has a beneficial effect on coefficient of performance.	[62]
Same as Fig. 30	68–75	68–75	30	104–115	H_2O/LiBr			0.173–0.438	Industrial waste heat	Increase in COPET by increasing the original heat source temperature, via recycling latent heat energy from the water purification process	[63,64]
Same as Fig. 30	60–80	60–80	10–40	100	(LiBr+LiI+$LiNO_3$+LiCl)+H_2O	–	20–40	≈ 0.25–0.5	Waste heat	better performance compared with the system using water-LiBr	[65]
Fig. 31	69–71	69–71	32	102–112	H_2O/LiBr	33–41	?	0.195–0.473	Hot water	110.3% performance increase, been highest amongst the 3 configurations.	[66]
Fig. 32	69–71	69–71	32	102–112	H_2O/LiBr	33–41	?	0.210–0.473	Hot water	61.5% performance increase, lowest.	[66]
Fig. 33	69–71	69–71	32	102–112	H_2O/LiBr	33–41	?	0.195–0.473	Hot water	79.3% performance increase, lower than case a, but higher than case b.	[66]
Same as Fig. 33	77.3–84.3	81.5–92.2	23.1–28.5	96.0–100.8	H_2O/LiBr	8.6–14.5		0.156–0.258	Hot water	A decisive role played by the mass flow rate of water supplied to the generator since COP can be increased up to 38%.	[67]
Fig. 34	60–80	60–80	20–25	100_{max}	H_2O/LiBr	15–20		0.30–038	Hot water	Recovery ratio 0.17–0.23 (5 kW input generator)	[68]
Parallel Waste heat supply	47	47	1–6	70	H_2O/LiBr	10		0.452	Industrial waste heat	Waste temperature from data centers is upgraded.	[70]
Fig. 36	124.3	124.3	35	174.0	H_2O/LiBr	20		0.47	Hot air	Total system's efficiency is 42%	[71]
Fig. 37	124.0	124.0	35	174.0	H_2O/LiBr	20		0.47	Hot air	Efficiency greater than case shown in Fig. 35(43%)	[71]
Fig. 38	92.2	92.2	35	110.0	H_2O/LiBr	20		0.49	Hot air	Highest system efficiency compared to Fig. 35 and 36(46%)	[71]

Another study was carried out by Zhuo and Machielsen [65] about the AHTs performances with Alkitrate as the working fluid. It was found that the COP values of the system were higher than or same as those of H_2O/LiBr under the same operating conditions. The alkitrate can be used for the higher temperature absorption heat transformers up to 260 °C. Iyoki et al. [66] described a study about physical properties (density, vapor pressure, viscosity, surface tension, and solubility) and thermal properties (heat capacities and heat of mixing). The measured properties showed good characteristics for absorption heat transformer. Yin et al. [67] proposed a comparative study for AHT utilizing working fluids consisting of TFE(2,2,2-triuoroethanol)/NMP(N-methy1-2-pyrrolidone), TFE/E181(dimethylethertetraethylene glycol), TFE/PYR (2-pyrrolidone), and H_2O/LiBr. When the output temperature was below 150 °C, the H_2O/LiBr was superior to others, but TFE/NMP, TFE/E181, and TFE/PYR showed better performance at higher temperature (up to 200 °C). He et al. [68] recommended 1,3-dimethylimidazolium dimethylphosphate ([MMIM][DMP])+ water/ethanol/methanol mixtures, which are ionic liquid mixtures, as working fluids in absorption cycles. The results exhibited that these binary solutions were noble candidates for these cycles due to their characteristics such as negative deviation of vapor pressure from Raoults law, and the excess enthalpy of these solutions was negative. Srinivas et al. [69] explored water-based AHT systems for desalination purposes using multi-effect distillation (MED) with different working fluid mixtures. The lists of mixtures used were as follows:

(1) [H_2O/LiBr], (2) [H_2O/LiI], (3) [H_2O/LiCl], (4) [H_2O/LiBr + LiI (4:1)], (5) [H_2O/LiCl + $LiNO_3$(2.8:1)], (6)[H_2O/LiBr + $LiNO_3$(4:1)], (7) [H_2O/LiBr + $ZnBr_2$(2:1)], (8) [H_2O/LiBr + LiI + $C_2H_6O_2$(3:1:1)], (9) [H_2O/LiBr + LiCl + $ZnCl_2$(3:1:4)], (10) [H_2O/LiBr + $ZnCl_2$ + $CaBr_2$ (1:1:0.13)], (11) [H_2O/LiBr + $ZnBr_2$ + $LiCl_2$(1:1.8:0.26)], (12) [H_2O/$LiNO_3$ + KNO_3 + $NaNO_3$(53:28:19 wt)], (13) [H_2O/LiCl + $CaCl_2$ + Zn$(NO_3)_2$ (4.2:2.7:1)], (14) [H_2O/LiBr + $LiNO_3$LiI + LiCl (5:1:1:2)].

Table 4
Utilized working fluids in AHTs.

Working pair	Ref. no.	Remarks
H_2O/Carrol mixtures	[83]	• Theoretically works over a large range of generator and evaporator temperature • Higher solubility, ECOP and gross temperature lift than H_2O/LiBr.
H_2O/LiCl H_2O/$CaCl_2$	[72,84]	• Environmentally friendly • Low cost • Lithium chloride solutions are not practical at an absorber temperature of 45 °C or higher due to solubility limitations
H_2O /(LiBr/LiI/$LiNO_3$/LiCl)	[65]	• Higher system performance than H_2O/LiBr • Wide range of solubility
Alkitrate	[73]	• Working at high temperature up to 260 °C. • Higher COP than H_2O/LiBrs • Limited in low temperature due to solubility problems
H_2O/LiBr + $LiNO_3$	[74]	• Appropriate physical an thermal properties for AHT
TFE/NMP	[49,75]	• High thermal stability • High output heat temperature • Flat vapor pressure curve • Strong negative deviation from Raoult's law • Wide operating conditions with no crystallization • Low working pressure
TFE/E181	[50,75,85,86]	• High thermal stability • High output heat temperature • Flat vapor pressure curve • Strong negative deviation from Raoult's law • Thermally stable up to 250 °C • Non-corrosive • Completely miscible
TFE/PYR	[87]	• High thermal stability • High output heat temperature • Flat vapor pressure curve • Strong negative deviation from Raoult's law
([MMIM][DMP]) + water/ethanol/methanol	[76]	• Negative deviation of vapor pressure from Raoult's law • Negative excess enthalpy
H_2O/LiBr-Lil	[78]	• Appropriate heat capacity
H_2O/LiBr + ZnBq + LiC1	[79]	• Appropriate vapor pressure
TFE_TEGDME	[82]	• Non-corrosive • Completely miscible over a wide range of temperature • Thermally stable up to 250 °C • Low working pressure • Low thermal conductivity

The results showed that among these combinations the highest COP of 0.56 was achieved by $H_2O/LiCl+LiNO_3$ mixture, while the highest distilled water output of 16 m^3/h was achieved by $H_2O/LiCl+CaCl_2+Zn(NO_3)_2$. Iyoki et al. [70,71] developed the approach of heat capacities evaluating water–lithium bromide–lithium iodide (H_2O/LiBr/LiI) systems, and the vapor pressure of the water–lithium bromide–zinc bromide–lithium chloride system. The results, which were in good agreement with experimental data, indicated that the heat capacities and vapor pressure of these systems would be very useful for the research and design of absorption heat transformers. Iyoki and Uemura [72] carried out a theoretical study about different absorption cycles with working pairs of water–lithium bromide–zinc chloride–calcium bromide ($H_2O/LiBr/ZnCl_2/CaBr_2$). The obtained COPs showed that this working fluid is appropriate for two-stage AHTs. Romero and Silva-Sotelo [73] explored a theoretical comparison of the two methods for determination of the absorbent concentration of lithium bromide in a solar absorption thermal system like absorption heat transformers or air conditioning systems. The two techniques used to correlate the concentrations were based on thermal conductivity and refractive index. It was found out that the refractive index has less error than that of other techniques. The in-line determination of LiBr concentration provided the possibility to improve optimal recovery of solar heat in absorption heat transformer systems. Coronas et al. [74] conducted a study about the thermodynamic properties of pure compounds TFE and TEGDME, and the binary mixtures needed to study the performance of the absorption cycles. They stated that the low thermal conductivity and enthalpy of evaporation of TFE could be improved by using the TFE/H_2O mixtures as a refrigerant instead of pure TFE. Table 4 summarizes the working fluids studied by researchers in AHTs.

6. Crystallization risk

LiBr is a salt, and in its solid state, it has a crystalline structure. There is a specific minimum solution temperature for any given LiBr salt concentration below which the salt begins to leave the solution and crystallize. Lithium bromide strong solution entering the absorber tends to crystallize when the absorber temperature is increased for a fixed evaporating pressure [51,75,76]. So it is considered as a key technical barrier for the development of water/LiBr AHTs. There are several approaches to avoid the crystallization problem, such as chemical crystallization inhibitors, heat and mass transfer enhancement, and thermodynamic cycle modification.

Bourouis et al. suggested water–(LiBr/LiI/$LiNO_3$/LiCl) as the working pair in an AHT for desalination purpose [57]. They concluded that the multicomponent salt mixture shows considerably higher solubility than that of the conventional working fluid H_2O/LiBr, is less corrosive, and the temperature of crystallization is 30 °C less than that of LiBr solution. Rivera et al. [13] reported similar results for water/Carrol™ as the working pair in a single stage absorption heat transformer, and concluded that water/Carrol™ could even be a better alternative mixture.

Shiming et al. [39] utilized TFE/NMP in a self-regenerated absorption heat transformer. Its most advantageous feature was the wide working range as a result of the absence of crystallization, but on the other hand, it had some negative features like lower boiling temperature difference between TFE and NMP, which made it a necessity for using a rectifier.

Zhao et al. [40] employed TFE/E181 as the working-pair in a double effect absorption heat transformer, which was non-corrosive, completely miscible, and thermally stable up to 250 °C. In addition to the mentioned benefits, the large difference in boiling temperatures between TFE and E181 made it a suitable candidate for AHT cycles. The additives 1-octanol and 2-ethyl-1-hexanol were used in a single-stage heat transformer utilizing H_2O/LiBr, by Rivera et al. [14]. The results showed that at the same conditions, absorber temperatures increased about 58 °C by adding 400 ppm of 2-ethyl-1-hexanol to the lithium bromide mixture. Also, it was shown that the coefficient of performance increases up to 40% with the same additive. The major disadvantage of this working pair was its propensity to crystallize at high lithium bromide concentrations. Simulation of a single-stage absorption heat transformer using a new working pair composed of ionic liquids and water (H_2O+[EMIM][DMP]) was performed by Zhang et al. [11]. In order to evaluate the new working pair, the simulation results were compared with those of (H_2O+LiBr) and (TFE/E181). The excellent cycle performance together with the advantages of negligible vapor pressure, no crystallization, and weak corrosion tendency to iron–steel materials might have made the new working pair better suited for the industrial absorption heat transformers. Wang et al. [75] investigated and compared two flow configurations of (H_2O+LiBr) AHT, which was used for water heating to evaluate the allowable operating conditions for each. The simulation results indicated that introducing the process water through the absorber firstly results in lower absorber temperature, and hence less tendency for crystallization. Parham et al. [77] proved that some modifications on the configuration of AHT could decrease the possibility of crystallization.

7. Performance evaluation by applying different models

Estimating and measuring the coefficient of performance (COP) in absorption heat transformer cycles are important issues for improvement and optimization of the performance of real AHT, for which many studies have been carried out by researchers. Hernandez et al. [78] performed a theoretical comparison study between a neural network model (NnM) and thermodynamic model (ThM) for on-line calculation of COP in an absorption heat transformer integrated with a water purification process (AHT-WP). Both models have their own advantages and disadvantages. The ThM model, which has been designed for steady-state conditions can precisely predict the physical properties and a wide range of any particular conditions; at the same time it is an appropriate choice for designing an AHT-WP using low temperature waste heat recovery. In addition, the COP calculated by ThM is a key to ensure reaching this value experimentally. The considerations for the NnM model are 16 on-line measured values, with 55 adjusted parameters (weights and biases), and two transfer functions (hyperbolic tangent and linear), which include the effect of heat losses and pressure drops into tubing and components that can be used in transitory and steady states. Simplicity of NnM due to the simulation by simple arithmetic operations is an advantage of this method. It is also very accurate for experimental COP agreement and for on-line calculation of COP. The NnM shows better correlations beside ThM, but it has a small range of operating conditions. Sencan et al. [79] described methodologies such as linear regression (LR), pace regression (PR), sequential minimal optimization (SMO), M5model tree, M5′ rules, decision table, and back propagation neural network (BPNN) to model COP of an AHT applied for increasing the low temperature values in a real small experimental solar pond. A comparison of R2 values for predicted COP of different algorithms indicates that BPNN has the largest values of 0.99 which can be considered reasonable. Hernandez et al. [80] suggested the application of an artificial neural network inverse (ANNi) model in order to predict the COP of the water purification of a process integrated to a heat transformer with energy recycling.

The specifications of this model are as follows: 16 neurons as input, 3 neurons as hidden layer, one layer as output, a feed forward with one hidden layer, a Levenberg–Marquardt learning

algorithm, a hyperbolic tangent sigmoid transfer function, and a linear transfer function. On the validation data set, simulations and experimental data tests were found to be in good agreement ($R > 0.99$). This model is considered to predict the optimal operating conditions such that by applying this methodology it is possible to obtain any unknown input variable which is the key to have an ideal COP. Velazquez et al. [81] developed a number of different algorithms simulated in MATLAB for predicting the LiBr concentration and estimating the COP of a water purification process integrated to an absorption heat transformer (WP-AHT). The validation of these algorithms, approved by five tests performed on the (AHT-WP), shows an absolute maximum of 1%. These algorithms can reduce the cost of the energy production and allow a control process. The calculation time of this process is 0.5 s. Escobar et al. [82] designed an on-line indirect measurement for predicting the system performance of an (AHT-WP). These models were supported by direct measurements outlet temperature of components, two calculated pressure levels (AB-EV, GE-CO), and two calculated concentrations (absorber and generator outlet concentrations) of the working fluids; the measurement of these variables assists in determining the coefficient of performance. Due to the noise and stochastic variables of this process, a kalman filter is used to predict COP. In addition, to estimate the COP, Escobar et al. [83], in one of their other studies, described controlling the corrosive attack which is possible by measuring the electrochemical potential and electrochemical current. The results of this work, which are similar to out-line steady estimations, are helpful in reducing the operation costs, applying an operating strategy, and testing new configurations. Hernandez et al. [84] reported a predictive model for WPAHT in order to obtain on-line prediction of the COP using an artificial neural network. Their study compared the COP with and without energy recycling. The network had additional two separate feed forward networks with one hidden layer which were used for increased values of COP with energy recycling and the COP values without energy recycling. The properties of this network are as follows: Levenberg–Marquardt learning algorithm, the hyperbolic tangent sigmoid transfer-function, and the linear transfer function were used. The results indicated that the simulation data and experimental data were in a good agreement ($R^2 > 0.99$). Colordo et al. [85] developed a study by using error propagation from the Monte Carlo method to the COP of the water purification system integrated to an AHT predicted by ANN. The Monte Carlo method offers a reasonable approach to error propagation of COP, in spite of the computing complexity. The accuracy of this method is confirmed by comparing the experimental and simulated results, and also the simulated results developed a new correlation for error propagation of COP prediction. The performance of ejector-absorption heat transformers (EAHTs) is predicted by Sozen et al. [86] by applying an ANN model. The network used Scaled Conjugate Gradient (SCG), Levenberg–Marquardt (LM) learning algorithms, and a logistic sigmoid transfer-function. The advantages of the ANN compared with classical methods were speed, simplicity, and capacity to learn from examples. So, engineering effort could be reduced. The model could predict the system's performance such as coefficient of performance (COP), exergetic coefficient of performance (ECOP), and circulation ratio (f). The study showed that the ANN model could be a good choice for determining the performance of the AHT systems instead of mathematical models. Sozen and Arcaklioglu [87] presented a study about determination of exergy analysis of an ejector-absorption heat transformer (EAHT) using an artificial neural network (ANN) model. Due to the complexity of exergy analysis of AHT, the ANN model was proposed for this system, which could deal with complicated situations. The best statistical coefficient (R^2 values) for training data equals to 0.999715, 0.995627, 0.999497, and 0.997648 by different algorithms with seven neurons for the non-dimensional exergy losses of evaporator, generator, absorber, and condenser, respectively. So the ANN can be used for the design and optimization of new or more complicated systems. Another way of determining the performance of the system is to predict the model by establishing a generalized heat transfer law $Q \sim \Delta\ (T_n)$. Qin et al. [88] derived a general relation between the COP and the heating load by applying the heat transfer law $Q \sim \Delta\ (T_n)$ $(n \neq 0)$, which considered the effect of heat transfer resistance, heat leak, and internal irreversibilities. The results of this relation were about the maximum COP, the corresponding heating load, optimal working temperature conditions, and optimal heat transfer surface area. The results could be a direction to find an optimal design for real absorption heat transformers. Chen et al. [89] suggested a study about modeling an irreversible four-temperature-level AHT by considering finite-heat capacity heat reservoirs, heat leakage, heat resistance, and internal irreversibility losses. The COP of real absorption heat transformers were optimized and analyzed by applying finite-time thermodynamics. The agreement between engineering design results and results obtained from relations was high, with deviation less than 3%. Relations showed the general relation between heating load and the COP, the characteristics of COP, and optimal heat transfer surface area. The results indicated that the COP would increase 1% if the heat transfer surface area distribution was optimized, and would increase about 23% if the internal irreversibility tended to unity and the heat leakages tended to zero. Escobar et al. [90] explored an experimental study about water purification system integrated to a single stage absorption heat transformer with energy recycling. The components of the absorption heat transformer consist of a helical double-pipe vertical evaporator, a helical double-pipe vertical condenser, an absorber, and a generator. They predicted the COP by applying a theoretical evaporator model which was incorporated into a thermodynamic model. This coupling model (theoretical and thermodynamic) could provide the opportunity to estimate the COP on-line, considering changes in the evaporator, and it led to control studies about the process. Colorado-Garrido et al. [91] proposed a numerical model of heat transfer and fluid dynamic behavior of a helical double-pipe evaporator used in an absorption heat transformer integrated to the water purification process. This model showed that the principle operation variable had an impact on the evaporator with the objectives of future control, design, optimization, and on-line estimation of COP. Kim and Infante Ferreira [92] reported an analytical study about single absorption cycles (absorption chillers, absorption heat pumps, absorption heat transformers) with and without refrigerant circulation. The model was developed by solving the governing equations, Duhring equations, and thermodynamic principles for mixtures. At the same time, it had the ability of describing the behavior of the absorption cycles like COP with minimal number of characteristic constants. A four-heat-reservoir absorption heat-transformer cycle was used by Sun et al. [93] to analyze the ecological optimal performance of an endoreversible absorption heat-transformer assuming a linear (Newtonian) heat transfer law. Using fundamental relationships derived by Qin et al. [94] and a derived ecological criterion, a numerical example was used to analyze the ecological performance and the effects of the cycle parameters on the ecological characteristics of the cycle. Results showed that the ecological criterion has long-term significance for optimal design of absorption heat transformers.

Ishida and Ji [95] performed a study about exergy analysis for single stage analysis by applying the graphical exergy methodology based on energy utilization diagrams (EUDs). Two cases with different flow ratios were investigated, and the results showed the effect of flow ratio on exergy losses, the lower flow ratio increases

the premixing exergy loss in the absorber. The EUD methodology was found to be a useful tool for predicting and analyzing the AHT.

8. Economic aspects

Smolen and Budnik-Rodz [96,97] presented a study about technical and economic aspects of different low temperature heat use systems, which included an absorption heat transformer. The investment cost and economic analysis of AHT were estimated on the basis of comparable absorption heat pump installation, due to the reason that this was a new technology and there are no technical installations on the market. They suggested that high efficiency of energy transformation does not mean economic profitability, and it depends on the proposed technical variant and a positive capital value which was possible by a standard interest rate and amortization period. Total heat transfer area of the real absorption heat transformers was a vital issue for the investment costs of the systems; therefore, heat transfer is of distributions that should be optimized [88].

Zhang et al. [98] proposed an investigation about absorption heat transformer and flash evaporator to decrease the consumption of CO_2 capture processes. By comparing the mentioned system with base CO_2 capture system it was found out that energy saving is about 2.62%. Also by performing an economic analysis they concluded that the annual profit was about 2.94 million RBM Yuan and the payback period is approximately 2.4 years. Ma et al. [9] performed an economical analysis on an industrial-scale absorption heat transformer in China with the aim of heat recovery from waste heat of synthetic rubber plant of Yanshan Petrochemical Corporation, Beijing, China. By applying this heat recovery system the steam consumption per ton of rubber plant decreased from 2.53 to 1.04 which resulted in 3.458 million Yuan (RMB) profit per year. Also the static payback period was about 2.01 years.

Jana [99] conducted a study about reviewing advances in heat pump assisted distillation column. The study covered both thermodynamic and economic aspects of different studies on absorption heat pump and absorption heat transformer.

9. Conclusion

Environmental issues and energy saving concerns have always been a major global problem. Absorption cycles can play an important role due to their capability of reducing discharge and reusing large amounts of industrial waste heat. A review of major technologies of absorption heat transformers comprising their varieties, applications, crystallization risk, working fluids, and performance evaluation by applying different models, and economic aspects was presented.

Besides the reduction of energy consumption and, thereby, overall cost, the AHT systems can be considered as an appropriate heat source for several industrial applications, because of their simple structure and operation and the supreme characteristic that is boosting mid or low-level heat sources such as industrial waste heat and renewable energy sources such as solar and geothermal, to higher levels. Through this review paper, we hope to convey one key message that further efforts in improving the absorption heat transformer technology will optimize the energy use and reduce the carbon footprint of numerous chemicals, less CO_2 emission and decreasing potentially the possibility of ozone layer depletion. Finally, it will draw wider interest to the use of absorption heat transformers.

References

[1] Ayou DS, Bruno JC, Saravanan R, Coronas A. An overview of combined absorption power and cooling cycles. Renew Sustain Energy Rev 2013;21:728–748.
[2] Hassan HZ, Mohamad AA. A review on solar cold production through absorption technology. Renew Sustain Energy Rev 2012;16:5331–48.
[3] Jaruwongwittaya T, Chen GM. A review: renewable energy with absorption chillers in Thailand. Renew Sustain Energy Rev 2010;14:1437–44.
[4] Donnellan P, Byrne E, Cronin K. Internal energy and exergy recovery in high temperature application absorption heat transformers. Appl Therm Eng 2013;56:1–10.
[5] Horuz I, Kurt B. Single stage and double absorption heat transformers in an industrial application. Int J Energy Res 2009;33:787–98.
[6] Kurem E, Horuz I. A comparison between ammonia–water and water–lithium bromide solutions in absorption heat transformers. Int Commun Heat Mass Transf 2001;28:427–38.
[7] Khamooshi M, Parham K, Atikol U. Overview of ionic liquids used as working fluids in absorption cycles. Adv Mech Eng 2013;2013.
[8] Horuz I, Kurt B. Absorption heat transformers and an industrial application. Renew Energy 2010;35:2175–81.
[9] Ma X, Chen J, Li S, Sha Q, Liang A, Li W, et al. Application of absorption heat transformer to recover waste heat from a synthetic rubber plant. Appl Therm Eng 2003;23:797–806.
[10] Sotelo SS, Romero RJ. Improvement of recovery energy in the absorption heat transformer process using water-Carrol™ for steam generation. Chem Eng Trans 2009:317–22.
[11] Zhang X, Hu D. Performance analysis of the single-stage absorption heat transformer using a new working pair composed of ionic liquid and water. Appl Therm Eng 2012;37:129–35.
[12] Zebbar D, Kherris S, Zebbar S, Mostefa K. Thermodynamic optimization of an absorption heat transformer. Int J Refrig 2012;35:1393–401.
[13] Rivera W, Romero RJ, Cardoso MJ, Aguillón J, Best R. Theoretical and experimental comparison of the performance of a single-stage heat transformer operating with water/lithium bromide and water/Carrol™. Int J Energy Res 2002;26:747–62.
[14] Rivera W, Cerezo J. Experimental study of the use of additives in the performance of a single-stage heat transformer operating with water–lithium bromide. Int J Energy Res 2005;29:121–30.
[15] Rivera W, Martínez H, Cerezo J, Romero RJ, Cardoso MJ. Exergy analysis of an experimental single-stage heat transformer operating with single water/lithium bromide and using additives (1-octanol and 2-ethyl-1-hexanol). Appl Therm Eng 2011;31:3525–32.
[16] Best R, Eisa MAR, Holland FA. Thermodynamic design data for absorption heat transformers-III. Operating on ammonia–water. Heat Recovery Syst CHP 1987;7:259–72.
[17] Best R, Rivera W. Thermodynamic design data for absorption heat transformers. Part six: operating on water-carrol. Heat Recovery Syst CHP 1994;14:427–36.
[18] Best R, Rivera W, Hernández J, Holland FA. Thermodynamic design data for absorption heat transformers-Part 5. Operating on ammonia–sodium thiocyanate. Heat Recovery Syst CHP 1992;12:347–56.
[19] Best R, Rivera W, Piltowsky I, Holland FA. Thermodynamic design data for absorption heat transformers – part four: operating on ammonia–lithium nitrate. Heat Recovery Syst CHP 1990;10:539–48.
[20] Eisa MAR, Best R, Holland FA. Thermodynamic design data for absorption heat transformers – Part II: operating on water–calcium chloride. J Heat Recovery Syst 1986;6:443–50.
[21] Grover GS, Devotta S, Holland FA. Thermodynamic design data for absorption heat transformers – Part III: operating on water–lithium chloride. Heat Recovery Syst CHP 1988;8:425–31.
[22] Patil KR, Chaudhari SK, Katti SS. Thermodynamic design data for absorption heat transformers – part III: operating on water–lithium iodide. Heat Recovery Syst CHP 1991;11:361–9.
[23] Rivera W, Romero RJ. Thermodynamic design data for absorption heat transformers – Part seven: operating on an aqueous ternary hydroxide. Appl Therm Eng 1998;18:147–56.
[24] Sözen A, Yücesu HS. Performance improvement of absorption heat transformer. Renew Energy 2007;32:267–84.
[25] Sözen A. Effect of irreversibilities on performance of an absorption heat transformer used to increase solar pond's temperature. Renew Energy 2004;29:501–15.
[26] Shi L, Yin J, Wang X, Zhu MS. Study on a new ejection–absorption heat transformer. Appl Energy 2001;68:161–71.
[27] Guo P, Sui J, Han W, Zheng J, Jin H. Energy and exergy analyses on the off-design performance of an absorption heat transformer. Appl Therm Eng 2012;48:506–14.
[28] Olarte-Cortés J, Torres-Merino J, Siqueiros J. Experimental study of a graphite disks absorber couple to a heat transformer. Exp Therm Fluid Sci 2013;46:29–36.
[29] Kotenko O, Moser H, Rieberer R. Thermodynamic simulation of alternative absorption heat pumping processes using natural working fluids. Int J Refrig 2012;35:594–604.
[30] Niang M, Cachot T, Goff PL. Evaluation of the performance of an absorption–demixtion heat pump for upgrading thermal waste heat. Appl Therm Eng 1998;18:1277–94.

[31] Alonso D, Cachot T, Hornut JM. Experimental study of an innovative absorption heat transformer using partially miscible working mixtures. Int J Therm Sci 2003;42:631–8.
[32] Rivera W, Best R, Hernández J, Heard CL, Holland FA. Thermodynamic study of advanced absorption heat transformers-I. Single and two stage configurations with heat exchangers. Heat Recovery Syst CHP 1994;14:173–83.
[33] Rivera W, Best R, Hernández J, Heard CL, Holland FA. Thermodynamic study of advanced absorption heat transformers-II. Double absorption configurations. Heat Recovery Syst CHP 1994;14:185–93.
[34] Zhao Z, Zhou F, Zhang X, Li S. The thermodynamic performance of a new solution cycle in double absorption heat transformer using water/lithium bromide as the working fluids. Int J Refrig 2003;26:315–20.
[35] Zhao Z, Ma Y, Chen J. Thermodynamic performance of a new type of double absorption heat transformer. Appl Therm Eng 2003;23:2407–14.
[36] Mostofizadeh C, Kulick C. Use of a new type of heat transformer in process industry. Appl Therm Eng 1998;18:857–74.
[37] Martínez H, Rivera W. Energy and exergy analysis of a double absorption heat transformer operating with water/lithium bromide. Int J Energy Res 2009;33:662–74.
[38] Ji J, Ishida M. Behavior of a two-stage absorption heat transformer combining latent and sensible heat exchange modes. Appl Energy 1999;62:267–81.
[39] Shiming X, Yanli L, Lisong Z. Performance research of self regenerated absorption heat transformer cycle using TFE-NMP as working fluids. Int J Refrig 2001;24:510–8.
[40] Zhao Z, Zhang X, Ma X. Thermodynamic performance of a double-effect absorption heat-transformer using TFE/E181 as the working fluid. Appl Energy 2005;82:107–16.
[41] Fartaj SA. Comparison of energy, exergy, and entropy balance methods for analysing double-stage absorption heat transformer cycles. Int J Energy Res 2004;28:1219–30.
[42] Parham K, Atikol U, Yari M, Agboola OP. Evaluation and optimization of single stage absorption chiller using ($LiCl+H_2O$) as the working pair. Adv Mech Eng 2013;2013.
[43] Rivera W, Cerezo J, Rivero R, Cervantes J, Best R. Single stage and double absorption heat transformers used to recover energy in a distillation column of butane and pentane. Int J Energy Res 2003;27:1279–92.
[44] Yari M. A novel cogeneration cycle based on a recompression supercritical carbon dioxide cycle for waste heat recovery in nuclear power plants. Int J Exergy 2012;10:346–64.
[45] Zare V, Yari M, Mahmoudi SMS. Proposal and analysis of a new combined cogeneration system based on the GT-MHR cycle. Desalination 2012;286:417–28.
[46] Yari M, Zare V, Mahmoudi S. Parametric study and optimization of an ejector-expansion TRCC cycle integrated with a water purification system. Proc. Inst. Mech. Eng., Part A: J. Power Energy 2013;227:383–98.
[47] Huicochea A, Romero RJ, Rivera W, Gutierrez-Urueta G, Siqueiros J, Pilatowsky I. A novel cogeneration system: a proton exchange membrane fuel cell coupled to a heat transformer. Appl Therm Eng 2013;50:1530–5.
[48] Sekar S, Saravanan R. Exergetic performance of eco friendly absorption heat transformer for seawater desalination. Int J Exergy 2011;8:51–67.
[49] Gomri R. Thermal seawater desalination: possibilities of using single effect and double effect absorption heat transformer systems. Desalination 2010;253:112–8.
[50] Gomri R. Energy and exergy analyses of seawater desalination system integrated in a solar heat transformer. Desalination 2009;249:188–96.
[51] Costa A, Bakhtiari B, Schuster S, Paris J. Integration of absorption heat pumps in a Kraft pulp process for enhanced energy efficiency. Energy 2009;34:254–60.
[52] Ishida M, Ji J. Proposal of humid air turbine cycle incorporated with absorption heat transformer. Int J Energy Res 2000;24:977–87.
[53] Huicochea A, Siqueiros J, Romero RJ. Portable water purification system integrated to a heat transformer. Desalination 2004;165:385–91.
[54] Romero RJ, Rodríguez-Martínez A. Optimal water purification using low grade waste heat in an absorption heat transformer. Desalination 2008;220:506–13.
[55] Siqueiros J, Romero RJ. Increase of COP for heat transformer in water purification systems – Part I: increasing heat source temperature. Appl Therm Eng 2007;27:1043–53.
[56] Romero RJ, Siqueiros J, Huicochea A. Increase of COP for heat transformer in water purification systems – Part II: without increasing heat source temperature. Appl Therm Eng 2007;27:1054–61.
[57] Bourouis M, Coronas A, Romero RJ, Siqueiros J. Purification of seawater using absorption heat transformers with water-($LiBr+LiI+LiNO_3+LiCl$) and low temperature heat sources. Desalination 2004;166:209–14.
[58] Huicochea A, Siqueiros J. Improved efficiency of energy use of a heat transformer using a water purification system. Desalination 2010;257:8–15.
[59] Huicochea A, Rivera W, Martínez H, Siqueiros J, Cadenas E. Analysis of the behavior of an experimental absorption heat transformer for water purification for different mass flux rates in the generator. Appl Therm Eng 2013;52:38–45.
[60] Sekar S, Saravanan R. Experimental studies on absorption heat transformer coupled distillation system. Desalination 2011;274:292–301.
[61] Duan L, Zhao M, Yang Y. Integration and optimization study on the coal-fired power plant with CO_2 capture using MEA. Energy 2012;45:107–16.
[62] Little AB, Garimella S. Comparative assessment of alternative cycles for waste heat recovery and upgrade. Energy 2011;36:4492–504.
[63] Little AB, Garimella S. Waste heat recovery in data centers using sorption systems. J Therm Sci Eng Appl 2012;4.
[64] Barragán Reyes RM, Gómez VMA, García-Gutiérrez A. Performance modelling of single and double absorption heat transformers. Curr Appl Phys 2010;10:S244–S248.
[65] Zhuo CZ, Machielsen CHM. Performance of high-temperature absorption heat transformers using alkitrate as the working pair. Appl Therm Eng 1996;16:255–262.
[66] Iyoki S, Yamanaka R, Uemura T. Physical and thermal properties of the water–lithium bromide–lithium nitrate system. Int J Refrig 1993;16:191–200.
[67] Yin J, Shi L, Zhu MS, Han LZ. Performance analysis of an absorption heat transformer with different working fluid combinations. Appl Energy 2000;67:281–92.
[68] He Z, Zhao Z, Zhang X, Feng H. Thermodynamic properties of new heat pump working pairs: 1,3-dimethylimidazolium dimethylphosphate and water, ethanol and methanol. Fluid Ph Equilib 2010;298:83–91.
[69] Srinivas G, Sekar S, Saravanan R, Renganarayanan S. Studies on a water-based absorption heat transformer for desalination using MED. Desalination Water Treat 2009;1:75–81.
[70] Iyoki S, Ohmori S, Uemura T. Heat capacities of the water–lithium bromide–lithium iodide system. J Chem Eng Data 1990;35:317–20.
[71] Iyoki S, Iwasaki S, Uemura T. Vapor pressures of the water–lithium bromide–zinc bromide–lithium chloride system at low temperatures. Ind Eng Chem Res 1989;28:1564–7.
[72] Iyoki S, Uemura T. Performance characteristics of the water–lithium bromide–zinc chloride–calcium bromide absorption refrigerating machine, absorption heat pump and absorption heat transformer. Int J Refrig 1990;13:191–6.
[73] Romero RJ, Silva-Sotelo S. Comparison of instrumental methods for in-line determination of LiBr concentration in solar absorption thermal systems. Sol Energy Mater Sol Cells 2006;90:2549–55.
[74] Coronas A, Vallès M, Chaudhari SK, Patil KR. Absorption heat pump with the TFE–TEGDME and TFE–H_2O–TEGDME systems. Appl Therm Eng 1996;16:335–45.
[75] Wang K, Abdelaziz O, Vineyard EA. The impact of water flow configuration on crystallisation in LiBr/H_2O absorption water heater. Int J Energy Technol Policy 2011;7:393–404.
[76] Garousi Farshi L, Seyed Mahmoudi SM, Rosen MA. Analysis of crystallization risk in double effect absorption refrigeration systems. Appl Therm Eng 2011;31:1712–7.
[77] Parham K, Yari M, Atikol UY. Alternative absorption heat transformer configurations integrated with water desalination system. Desalination 2013. http://dx.doi.org/10.1016/j.desal.2013.08.013.
[78] Hernández JA, Romero RJ, Juárez D, Escobar RF, Siqueiros J. A neural network approach and thermodynamic model of waste energy recovery in a heat transformer in a water purification process. Desalination 2009;243:273–85.
[79] Şencan A, Kizilkan O, Bezir NC, Kalogirou SA. Different methods for modeling absorption heat transformer powered by solar pond. Energy Convers Manag 2007;48:724–35.
[80] Hernández JA, Bassam A, Siqueiros J, Juárez-Romero D. Optimum operating conditions for a water purification process integrated to a heat transformer with energy recycling using neural network inverse. Renew Energy 2009;34:1084–91.
[81] Velazquez VM, Hernández JA, Juárez D, Siqueiros J, Mussati SF. On-line $LiBr+H_2O$ estimation for the performance of a water purification process integrated to an absorption heat transformer. Desalination Water Treat 2009;5:12–8.
[82] Escobar RF, Juárez D, Siqueiros J, Irles C, Hernández JA. On-line COP estimation for waste energy recovery heat transformer by water purification process. Desalination 2008;222:666–72.
[83] Escobar RF, Uruchurtu J, Juárez D, Siqueiros J, Hernández JA. On-line indirect measures estimation for the performance of an absorption heat transformer integrated to a water purification process. Meas: J Int Meas Confed 2009;42:464–73.
[84] Hernández JA, Juárez-Romero D, Morales LI, Siqueiros J. COP prediction for the integration of a water purification process in a heat transformer: with and without energy recycling. Desalination 2008;219:66–80.
[85] Colorado D, Hernández JA, El Hamzaoui Y, Bassam A, Siqueiros J, Andaverde J. Error propagation on COP prediction by artificial neural network in a water purification system integrated to an absorption heat transformer. Renew Energy 2011;36:1315–22.
[86] Sözen A, Arcaklioğlu E, Özalp M, Yücesu S. Performance parameters of an ejector-absorption heat transformer. Appl Energy 2005;80:273–89.
[87] Sözen A, Arcaklioğlu E. Exergy analysis of an ejector-absorption heat transformer using artificial neural network approach. Appl Therm Eng 2007;27:481–491.
[88] Qin X, Chen L, Sun F. Performance of real absorption heat-transformer with a generalized heat transfer law. Appl Therm Eng 2008;28:767–76.
[89] Chen L, Qin X, Sun F. Model of irreversible finite-heat capacity heat reservoir absorption heat transformer cycle and its application. Proc Inst Mech Eng, Part C: J Mech Eng Sci 2007;221:1643–51.
[90] Escobar RF, Hernández JA, Astorga-Zaragoza CM, Colorado D, Juárez D, Siqueiros(J.). Analysis of the evaporator heat flow rate in a water purification process integrated to an absorption heat transformer with energy recycling. Desalination Water Treat 2009;5:59–67.
[91] Colorado-Garrido D, Santoyo-Castelazo E, Hernández JA, García-Valladares O, Siqueiros J, Juarez-Romero D. Heat transfer of a helical double-pipe vertical

evaporator: theoretical analysis and experimental validation. Appl Energy 2009;86:1144–53.
[92] Kim DS, Infante Ferreira CA. Analytic modelling of steady state single-effect absorption cycles. Int J Refrig 2008;31:1012–20.
[93] Sun F, Qin X, Chen L, Wu C. Optimization between heating load and entropy-production rate for endoreversible absorption heat-transformers. Appl Energy 2005;81:434–48.
[94] Qin X, Chen L, Sun F, Wu C. An absorption heat-transformer and its optimal performance. Appl Energy 2004;78:329–46.
[95] Ishida M, Ji J. Graphical exergy study on single stage absorption heat transformer. Appl Therm Eng 1999;19:1191–206.
[96] Smolen S, Budnik-Rodz M. Technical and economic aspects of waste heat utilisation. Therm Sci 2007;11:165–72.
[97] Smolen S, Budnik-Rodz M. Low rate energy use for heating and in industrial energy supply systems – some technical and economical aspects. Energy 2006;31:2252–67.
[98] Zhang K, Liu Z, Li Y, Li Q, Zhang J, Liu H. The improved CO_2 capture system with heat recovery based on absorption heat transformer and flash evaporator. Appl Therm Eng 2014;62:500–6.
[99] Jana AK. Advances in heat pump assisted distillation column: a review. Energy Convers Manag 2014;77:287–97.